SPACE CURRENT DIVISION IN SMALL PENTODES

BY

JAMES DARR, JR.
and
SOLOMON MANBER

1948

SUBMITTED IN PARTIAL FULFILLMENT OF THE

REQUIREMENTS FOR THE DEGREE OF

BACHELOR OF SCIENCE

From the
MASSACHUSETTS INSTITUTE OF TECHNOLOGY

1948

Signatures of Authors _____

_____

Signature of Professor
in Charge of Thesis _____

ACKNOWLEDGEMENT

The authors wish to express their appreciation to Professor Godfrey T. Coate for his assistance in clarifying the problem and for his suggestions of possible methods for its solution.

TABLE OF CONTENTS

SUMMARY

It was the purpose of the experimenters to attempt to produce the static characteristics for small pentodes by developing functions of space current division at the electrodes.

When operating pentodes within the normal range of electrode voltages, changes in plate potential affect the total space current and its division between the screen and control grid very little. Moreover, although the total space current is controlled largely by the control grid, the division of the space current between the screen and the plate is affected very little by the control grid potential.

Taking into account the effects of initial velocities and contact potentials, and making use of the above facts, it is possible to express the electrode currents in terms of the three-halves power of a corrected electrode potential and an empirical function. Methods for obtaining the electrode correction voltages and the empirical functions for pentodes will be presented in this paper.

INTRODUCTION

The need for elaborate and costly equipment to determine the complete static characteristics of power triodes motivated E. L. Chaffee[1] to investigate the division of space current in power triodes. From the results of his investigation, he was able to determine those portions of the static curves in the regions in which the maximum dissipations of the tube would normally be exceeded using ordinary direct current methods.

By an extension of Chaffee's methods, Clifford M. Wallis[2] developed a method for determining the space current division in the power tetrode. It is the purpose of this paper to describe a process of further extending Chaffee's and Wallis' method for the determination of space current division between the electrodes of small pentodes.

Since, for small pentodes, it is possible to determine static characteristics by direct current measurements, the results of this paper are of academic interest only. It is highly probable, however, that this method in its entirety can be applied to large power pentodes where it would be of practical importance.

- -

[1]Chaffee, E. L. "The Characteristic Curves of a Triode." Proceedings of the I.R.E., Volume 30, Number 8 (August, 1942), 383-395.

THEORETICAL DISCUSSION

In Langmuir and Compton's[3] paper, it was shown that Child's 3/2 power law (see Figure 1) should be modified by a correction voltage to account for initial electron velocities and contact potential. If, then, we write Child's Equation as

(1) $i = A(V + V_t)^{3/2}$, (see Figure 2)

the current at every point within a vacuum tube is

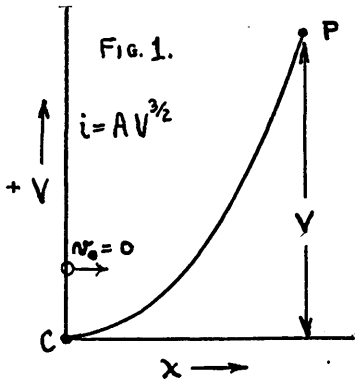

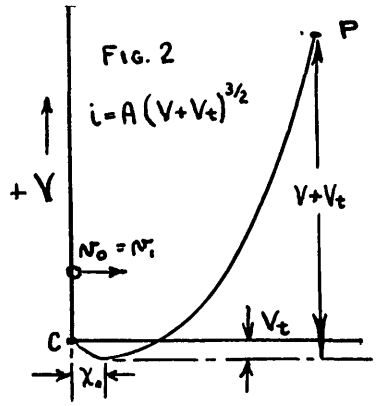

represented, provided $(V + V_t)$ everywhere is altered proportionately. If $(V + V_t)$ in all space within a vacuum tube is changed by a constant factor (G), the current at all electrodes will be changed by $(G)^{3/2}$.

Considering the space just outside the cathode as the plane from which V is measured, the following

- -

[2]Wallis, Clifford M. "Space Current Division in the Power Tetrode." Proceedings of the I.R.E., Vol. 35, Number 4 (April, 1947) 369-377.

[3]Langmuir, Irving and Compton, K.T. "Electrical Discharges in Gases." Reviews of Modern Physics, Volume 3 (April, 1931) 237-257.

equations must apply in order to change $(V + V_t)$ by a factor (G) at all points:

$$
\begin{aligned}
&\text{(a)}\quad e_g' + \phi_c - \phi_g + V_t = G(e_g + \phi_c - \phi_g + V_t)\\
&\text{(b)}\quad e_s' + \phi_c - \phi_s + V_t = G(e_s + \phi_c - \phi_s + V_t)\\
&\text{(c)}\quad e_{su}' + \phi_c - \phi_{su} + V_t = G(e_{su} + \phi_c - \phi_{su} + V_t)\\
&\text{(d)}\quad e_p' + \phi_c - \phi_p + V_t = G(e_p + \phi_c - \phi_p + V_t)
\end{aligned}
\qquad (2)
$$

The ϕ's in the above equations are used to represent the electron affinities of the electrode materials, and the potentials marked (') are the measured electrode potentials corresponding to the conditions that $V' + V_t = G(V + V_t)$. In the remainder of this paper, $\phi_c - \phi_g + V_t$ will be represented by Δe_g, $\phi_c - \phi_s + V_t$ by Δe_s, $\phi_c - \phi_{su} + V_t$ by Δe_{su}, and $\phi_c - \phi_p + V_t$ by Δe_p. In order to change $(V + V_t)$ by a factor (G) at all points in space within the tube, $(e_g - \Delta e_g)$, $(e_s - \Delta e_s)$, $(e_{su} - \Delta e_{su})$ and $(e_p - \Delta e_p)$ must each be changed so that their ratios remain constant.

Division of the Space Current at the Control Grid

As can be seen in Figures 3 and 4, variations of the plate potentials of pentodes over a large range has little or no effect upon the potential distribution between the screen and cathode, and hence has little effect on the total space current. Until the plate potential becomes so low that the effective potential

at the suppressor grid plane becomes negative, the plate voltage has little effect on the total space current or its division between the screen and control grids. When the plate potential is lowered to

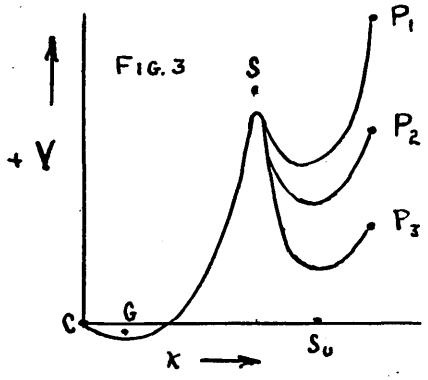

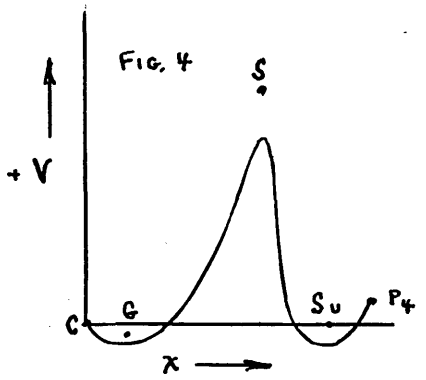

such a point, some of the electrons approaching the suppressor will lose all their forward velocity, and will be attracted back towards the screen. Part of this electron flow will pass through the screen and continue on towards the cathode, which effectively reduces the total space current and alters its division between the screen and control grids. The curves of the current ratio (i_g/i_o) versus plate potential on Plate I, plotted from experimental data on a 6SK7 pentode (used throughout the experiment), show little change in division ratio for variations in plate voltage over a large range.

Since the current density and potential distribution in the region between the cathode and screen grid are not materially changed by changes in plate potential, it is necessary only to satisfy equations

2 (a) and 2 (b) in order to change $V + V_t$ at all points in the grid-cathode region by some factor (G). If we are to satisfy these equations, $(e_g - \Delta e_g)$ and $(e_s - \Delta e_s)$ must be changed in such a manner that their ratio remains constant. If we call this ratio L_g, then

$$(3) \qquad L_g = \frac{e_g - \Delta e_g}{e_s - \Delta e_s} = \frac{e_{go}}{e_{so}} \ .$$

The curves of constant i_{sp} (plate plus screen current) and constant i_o (cathode current) in the e_{sp}-e_g plane (see Plate II) are analogous to the constant i_p and i_o curves of a triode in the e_p-e_g plane. Over a large region, these curves are parallel and straight, and may be written in terms of the corrected grid and screen voltages as follows:

$$(4) \qquad i_o' = B\left[(e_g - \Delta e_g) + \frac{(e_s - \Delta e_s)}{\mu_{gs}}\right]^{3/2}$$

$$= B\left[e_{go} + \frac{e_{so}}{\mu_{gs}}\right]^{3/2}$$

$$= B\left[\frac{e_{so}}{\mu_{gs}}\right]^{3/2}\left[1 + \mu_{gs}L_g\right]^{3/2}$$

where B is the perveance of the tube and $\mu_{gs} = -\left.\frac{\partial e_s}{\partial e_g}\right|_{i_o = \text{constant}}$

Δe_g and Δe_s may be determined easily from the constant i_o curves on Plate II as follows:

$$i_1 = B\left[e_{g1} - \Delta e_g + \frac{(e_{s1} - \Delta e_s)}{\mu_{gs}}\right]^{3/2}$$

$$(5) \quad i_2 = B\left[e_{g2} - \Delta e_g + \frac{(e_{s2} - \Delta e_s)}{\mu_{gs}}\right]^{3/2}$$

$$i_3 = B\left[e_{g3} - \Delta e_g + \frac{(e_{s3} - \Delta e_s)}{\mu_{gs}}\right]^{3/2}$$

For constant measured values of i_1, i_2, and i_3, the unknown, μ_{gs}, may be determined from the slope in the linear region. This leaves only B, Δe_g, and Δe_s as unknowns in equations (5). By simultaneous solution of the three equations, these constants may be determined.

Another method, which checks the one outlined above very closely, may be used. This method was used by Chaffee and Wallis in the case of triodes and tetrodes, and is illustrated on Plate II. If the ratio $(e_{go}/e_{so}) = L_g$ is held constant, the ratio of currents, (i_g/i_{sp}) will also be constant. Therefore, if several points are obtained on the e_{sp}-e_g plane for a constant value of i_g/i_{sp}, these points (P_1, P_2, P_3, and P_4) will lie on a constant L_g line. These constant L_g lines are straight and all pass through the point Δe_g and Δe_s. Hence the intersection of the lines determined by the constant ratios of i_g/i_{sp} will be the point Δe_g and Δe_s, and can be measured directly on the e_{sp}-e_g plane, as can be seen on Plate II.

Analytically, this may be shown by the following formulae:

$$(6) \qquad i_{sp2}/i_{sp1} = \left[\frac{e_{s2} - \Delta e_s}{e_{s1} - \Delta e_s}\right]^{3/2}$$

$$\text{or} \qquad i_{sp2}/i_{sp1} = \left[\frac{e_{g2} - \Delta e_g}{e_{g1} - \Delta e_g}\right]^{3/2}$$

from which

$$(7) \qquad \Delta e_g = \frac{e_{g1}(i_{sp2}/i_{sp1})^{2/3} - e_{g2}}{(i_{sp2}/i_{sp1})^{2/3} - 1}$$

$$\Delta e_s = \frac{e_{s1}(i_{sp2}/i_{sp1})^{2/3} - e_{s2}}{(i_{sp2}/i_{sp1})^{2/3} - 1}$$

where the subscripts (1) refer to the point P_1 and the subscripts (2) refer to the point P_2 on Plate II. The equations above were solved for all of the points on Plate II, and their values averaged. The average values of Δe_g and Δe_s found by this method agreed quite well with the values found by the other two methods.

At low values of screen potential, the curves of i_o on Plate II can be seen to vary from linearity, and this departure may be treated as an empirical

function of L_g. Equation (4) then becomes

$$(8) \quad i_o = B\left[\frac{e_{so}}{\mu_{gs}}\right]^{3/2}\left[1 + \mu_{gs}L_g\right]^{3/2} \cdot F(L_g)$$

In similar manner, recalling that the current division at the control grid is independent of the plate voltage, we may define $F_g(L_g)$ and $F_{sp}(L_g)$ as the current division factors operating on the "linear" cathode current to produce the actual i_g and i_{sp}. The following equations may now be written:

$$(10) \quad i_{sp} = B\left[\frac{e_{so}}{\mu_{gs}}\right]^{3/2}\left[1 + \mu_{gs}L_g\right]^{3/2} \cdot F_{sp}(L_g)$$

$$(11) \quad i_g = B\left[\frac{e_{so}}{\mu_{gs}}\right]^{3/2}\left[1 + \mu_{gs}L_g\right]^{3/2} \cdot F_g(L_g)$$

$$(12) \quad F_g(L_g) = F(L_g) - F_{sp}(L_g)$$

The curves of constant i_o, i_{sp}, and i_g are plotted on Plate III from experimental data, and constant L_g lines are plotted from the corrected origin. From the above definitions of $F(L_g)$, $F_{sp}(L_g)$, and $F_g(L_g)$, and the notations on Plate III, it follows that

$$(13) \quad F(L_g) = (e_{so}^{IV}/e_{so})^{3/2}$$

$$(14) \qquad F_{sp}(L_g) = (e_{so}^{IV}/e_{so}^{V})^{3/2}$$

$$(15) \qquad F_g(L_g) = (e_{so}^{IV}/e_{so}^{VI})^{3/2}$$

would be true if the curves on Plate III represented equal values of current. However, it was thought best to limit the grid current to a small value. It is therefore necessary to divide equation (15) by the ratio of i_o to i_g, which is 7.5.

Division of Space Current at the Screen Grid

Although the total space current is largely determined by the control grid potential, the division of this current between the screen and the plate is nearly independent of the control grid potential over the usual operating range. Experimental verification of the above statement is illustrated on Plate IV.

As can be seen from Plate V, the constant i_p and constant i_o (since e_g was negative, i_g was zero and $i_o = i_{sp}$) curves were straight and very nearly parallel to the plate potential axis. In this region, for any constant value of control grid potential, i_{sp} could be described by

$$(16) \qquad i_{sp} = C\left[e_{so}' + \frac{e_{po}'}{\mu_{sp}}\right]^{3/2}$$

when e_{su} is held at cathode potential (as was the case throughout the experimental work) and Δe_{su} is assumed to be negligible. In the above equation, e_{so}' and e_{po}' are the electrode potentials necessary to cause the same cathode, plate, and screen current if the grid were removed, and μ_{sp} is the slope of the constant i_{sp} curves in the e_p-e_s plane. Since these curves are nearly parallel to the plate potential axis, μ_{sp} is very large.

Equation (16) may also be written as

$$(16a) \qquad i_{sp} = C\left[\frac{e_{po}'}{\mu_{sp}}\right]^{3/2}\left[1 + \frac{\mu_{sp}}{L_p}\right]^{3/2}$$

where $L_p = e_{po}'/e_{so}'$.

Since $e_{so}' = e_s - \Delta e_s'$ and $e_{po}' = e_p - \Delta e_p'$, it is necessary to determine $\Delta e_s'$ and $\Delta e_p'$ in order to locate the potential origin on the e_p-e_s plane from which the 3/2 law is applicable.

Since μ_{sp} is large, i_{sp} is practically independent of e_{po}' when e_{so}' is appreciable as can be seen from equation (16). Solving equation (4) and equation (16) simultaneously will show the dependence of $\Delta e_s'$ on the control grid voltage, e_g.

$$(4) \quad i_o = B\left[e_{go} + \frac{e_{so}}{\mu_{gs}}\right]^{3/2}$$

$$(4a) \quad i_o = B/\mu_{gs}(e_{go}\mu_{gs} + e_s - \Delta e_s)^{3/2}$$

$$(16) \quad i_{sp} = i_o = C\left[e_{so}' + \frac{e_{po}'}{\mu_{sp}}\right]^{3/2}$$

m

$$(16a) \quad i_{sp} = i_o = C(e_s - \Delta e_s' + E)^{3/2}$$

where $E = e_{po}'/\mu_{sp}$ and is small

Therefore,

$$-\Delta e_s' + E = e_{go}\mu_{gs} - \Delta e_s$$

And

$$\Delta e_s' = (\Delta e_s + E + \Delta e_g\mu_{gs}) - \mu_{gs}e_g$$

$$\Delta e_s' = k_1 - \mu_{gs}e_g$$

where $k_1 = \Delta e_s + E + \Delta e_g/\mu_{gs}$ and is approximately a constant. Therefore, to a first approximation, $\Delta e_s'$ varies linearly with e_g.

Again, there are several methods of determining $\Delta e_s'$. It may be determined analytically by use of equation (16), as shown immediately below, for any constant value of control grid voltage.

$$i_{sp1} = C\left[e_{s1} - \Delta e_s' + \frac{e_{po1}}{\mu_{sp}}\right]^{3/2}$$

$$i_{sp2} = C\left[e_{s2} - \Delta e_s' + \frac{e_{po2}}{\mu_{sp}}\right]^{3/2}$$

Holding e_{po} constant, $e_{po1} = e_{po2}$, and letting $e_{po1}/\mu_{sp} = E$, which is small,

$$(18) \quad \Delta e_s' = \frac{e_{s2} - e_{s1}(i_{p1}/i_{p2})^{3/2}}{1 - (i_{p1}/i_{p2})^{3/2}} + E$$

Since E is small compared to the first term in equation (18), it may be neglected for all practical purposes. $\Delta e_s'$ was calculated by equation (18) for a number of control grid voltages, and the results plotted as curve "A" on Plate VII.

$\Delta e_p'$ and $\Delta e_s'$ were also determined by the method outlined by Wallis in his article on tetrodes, which is similar to the method for determination of the correction voltages for the control grid and the screen grid as outlined previously. This consists of determining a series of points in the e_p - e_s plane for each of several constant ratios of i_p to i_s. By locating the intersection of the lines drawn through each series of points, the origin on the e_p-e_s plane from which the 3/2 law is applicable is established.

These correction voltages may also be determined from the above points by analytical methods as shown below:

$$(19)\quad \Delta e_p' = \frac{e_{po1}(i_{p2}/i_{p1})^{2/3} - e_{po2}}{(i_{p2}/i_{p1})^{2/3} - 1}$$

$$(20)\quad \Delta e_s' = \frac{e_{so1}(i_{p2}/i_{p1})^{2/3} - e_{so2}}{(i_{p2}/i_{p1})^{2/3} - 1}$$

where the subscripts (1) refer to P_1 and subscripts (2) refer to P_2 on Plates VIII, IX, X, and XI.

Since the constant i_p and constant i_s curves are nearly vertical in the e_p-e_s plane in the usual operating range of plate potentials (see Plate V), it was impossible to locate points of constant i_p/i_s with any accuracy in this region. For this reason, it was necessary to locate these points of constant ratio in the region of low plate potentials where the plate current is largely controlled by the plate voltage. At these plate voltages, the field at the suppressor grid becomes negative, causing electrons to return towards the screen and cathode which reduces the total space current. Because the correction voltages must correct for space current, any screen correction voltage experimentally determined at low values of e_p would not be expected to agree in magnitude with values obtained at high plate potentials. The correction factors determined at these low plate potentials is also plotted on Plate VII, labeled Curve "B".

Nothing has been said as yet about $\Delta e_p'$, the plate correction voltage. While this was impossible to measure at high values of plate voltage, it will be shown later to be negligible in this region. In the region of low plate voltage where it was measured (described above), this correction voltage was found to be very small, and hence unimportant.

Plate VI shows the constant i_o and constant i_p curves on the e_p-e_g plane in the region in which they depart from linearity. Here the total space and electrode currents may be expressed in terms of the "linear" space current and empirically determined functions of L_p by the following equations:

$$(21) \quad i_{sp} = C\left[\frac{e_{po}'}{\mu_{sp}}\right]^{3/2}\left[1 + \frac{\mu_{sp}}{L_p}\right]^{3/2} \cdot F(L_p)$$

$$(22) \quad i_p = C\left[\frac{e_{po}'}{\mu_{sp}}\right]^{3/2}\left[1 + \frac{\mu_{sp}}{L_p}\right]^{3/2} \cdot F_p(L_p)$$

$$(23) \quad i_s = C\left[\frac{e_{po}'}{\mu_{sp}}\right]^{3/2}\left[1 + \frac{\mu_{sp}}{L_p}\right]^{3/2} \cdot F_s(L_p)$$

As can be seen from the above equations, along a line of constant L_p, i_{sp}, i_p, and i_s vary as the 3/2 power of e_{po}'. Using the notation on Plate VI, it follows that

$$(24) \quad F(L_p) = \left[\frac{e_{po}}{e_{pol}}\right]^{3/2}$$

$$(25) \quad F_p(L_p) = \left[\frac{e_{po2}}{e_{pol}}\right]^{3/2}$$

$$(26) \quad F_s(L_p) = F(L_p) - F_p(L_p)$$

From the foregoing equations and the data on Plate VI, the functions $F(L_p)$, $F_p(L_p)$ and $F_s(L_p)$ were plotted on Plate XII.

Since $L_p = e_{po}'/e_{so}'$, for high values of e_{po}', L_p is at least greater than unity. As can be seen from Plate XII, for L_p greater than one, $F(L_p)$ and $F_p(L_p)$ are very nearly constant. Hence, the value of $\Delta e_p'$ at high values of e_p has no effect on i_{sp} or its division between the electrodes. Since, as previously stated, Δe_p was found to be negligible for low plate voltages, it may now be disregarded over the whole range of e_p.

PRESENTATION OF RESULTS

For a given control grid potential and a given screen grid potential, Plate XIII may be used to determine the "linear" cathode current. This, in reality, is a graphical solution of equation (4)

which may be written in the form

$$(4) \quad i_o'^{2/3} = \frac{B^{2/3}}{\mu_{gs}} \left[\mu_{gs} e_{go} + e_s - \Delta e_s\right]$$

This solution is accomplished by plotting $i_o'^{2/3}$ on the ordinate against e_s on the abscissa, holding $\mu_{gs}e_{go}$ equal to zero. The value of $\mu_{gs}e_{go}$ is plotted versus e_g so that the vertical displacement from the abscissa equals the $\mu_{gs}e_{go}$ value. This distance, determined by e_g, is then added to the e_s value by a 45 degree projection. Plotting i_o' versus $i_o'^{2/3}$ on the same plate allows the "linear" cathode current to be read directly.

It is necessary to correct the cathode current by $F(L_g)$ for both positive and negative values of L_g. On Plate XIV, lines of constant $-L_g$ are drawn, and from the screen and grid potentials, it is possible, by interpolation, to determine $-L_g$ over the important range. The correction factor $F(-L_g)$ is plotted on this plate also, and when the i_o' from Plate XIII is multiplied by $F(-L_g)$, the actual i_o (in this region $i_o = i_{sp}$) is determined. The same procedure is followed on Plates XV and XVI for positive L_g values.

On Plate XVII, the experimental and calculated grid current for a screen voltage of 50 volts and a

plate voltage of 50 volts are plotted. The data for the calculated curve was obtained by multiplying the cathode current i_o' from Plate XIII by the factor $F_g(L_g)$ obtained from Plate XVI. These curves are very nearly parallel over the entire range of grid voltages. However, the theoretical curve shows slightly higher values of grid current than the experimental curve for the same grid voltage. It was found that increasing the screen voltage increased the total space current, but decreased the control grid division factor in such a manner as to offset the increase in total space current, so that the control grid current remained essentially constant over a wide range of screen voltages. In this respect, the theoretical curve showed the same properties as the experimental curve.

To determine the division factors $F(L_p)$, $F_p(L_p)$, and $F_s(L_p)$, it is necessary to determine L_p', which is dependent upon grid potential, screen potential, and plate potential. The dependency upon grid potential results from the fact that the screen correction voltage is a function of the grid voltage. On Plate XVIII, this correction voltage is plotted versus grid potential (taken from curve "A", Plate VI) in such a manner that the screen correction is equal to the distance from the ordinate. By means of projections,

this correction voltage is subtracted from the screen potential and L_p may be determined (since $e_p = e_{po}$).

Plate XIX is the same as Plate XVIII with the exception that the screen correction voltage curve "B" on Plate VI was used instead of curve "A". Although curve "A" is assumed to be the better curve, as a check, each was used in determination of the final results.

On Plates XX, XXI, and XXII, the experimentally determined curves of plate current, screen current, and cathode current are plotted along with the calculated curves. The two sets of calculated curves results from the use of curve A and curve B on Plate VI in determining L_p. In many places, the two curves overlapped, and at no point was there any large discrepancy. Both calculated curves predicted the knee of the curves and the magnitude of the currents as close, or closer, than the experimental curves of other 6SK7 pentodes.

CONCLUSION

The data used in this paper was compiled entirely from experiments on a single 6SK7 pentode. This tube was carefully selected to insure that its characteristics were typical of its class and the tube free of gas. While the results of this

experiment are not conclusive because the investigation was confined to a single tube, it is strongly felt by the experimenters, because of the positive results obtained, that the application of this method is not limited to this pentode alone. This, of course, would bear further investigation.

The presentation of empirical functions can be simplified greatly by plotting them on a log-log chart in a manner that allows complete static curves to be obtained for any grid, screen, or plate voltage within the normal operating regions. Such a method is outlined by Chaffee and Wallis in their articles on triodes and tetrodes.

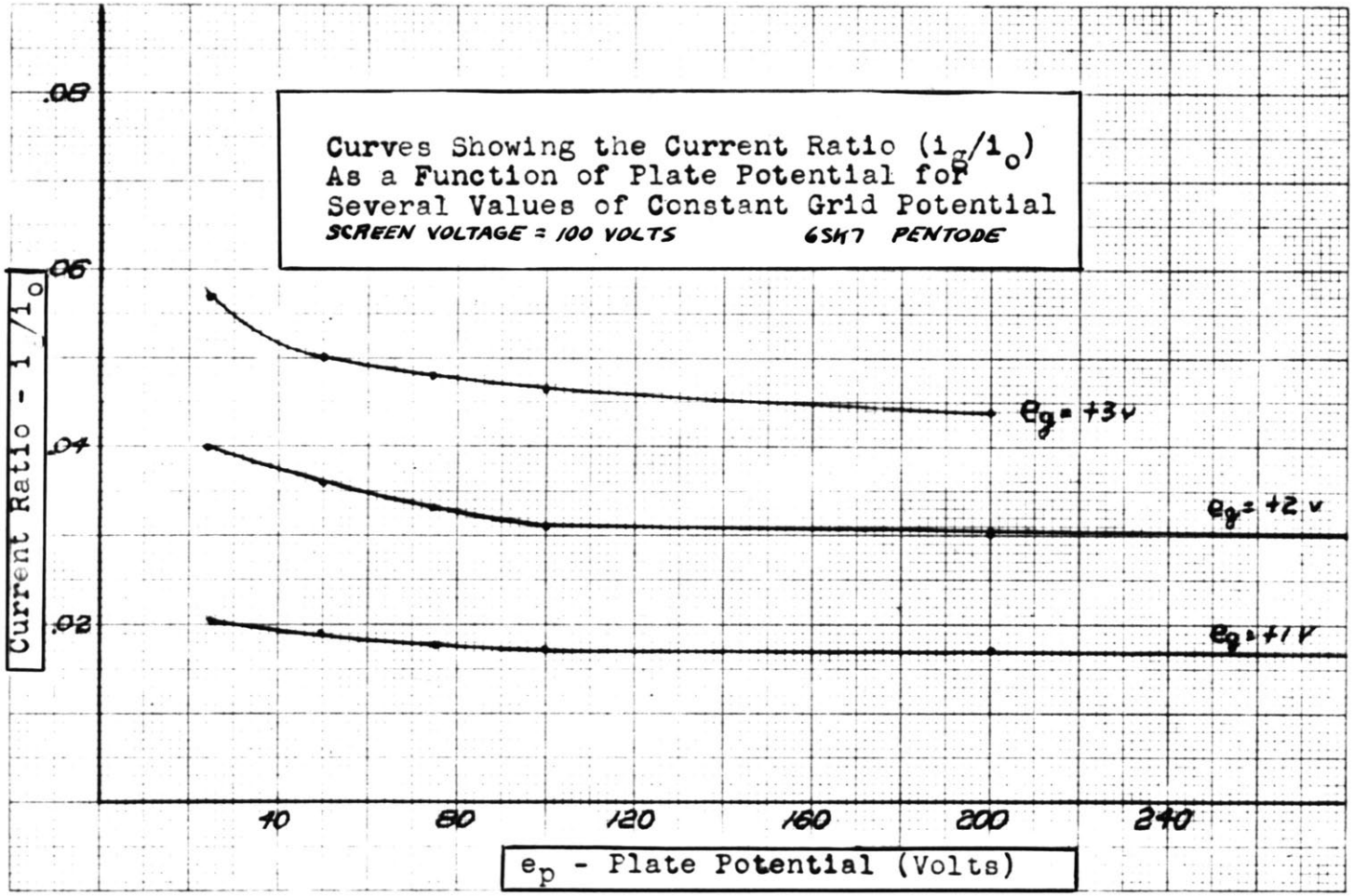
Curves Showing the Current Ratio (i_g/i_o)
As a Function of Plate Potential for
Several Values of Constant Grid Potential
SCREEN VOLTAGE = 100 VOLTS
6SK7 PENTODE
Current Ratio - i_g/i_o
.08
.06
.04
.02
e_g = +3 v
e_g = +2 v
e_g = +1 v
40
80
120
160
200
240
e_p - Plate Potential (Volts)

PLATE NO I

PLATE NO II

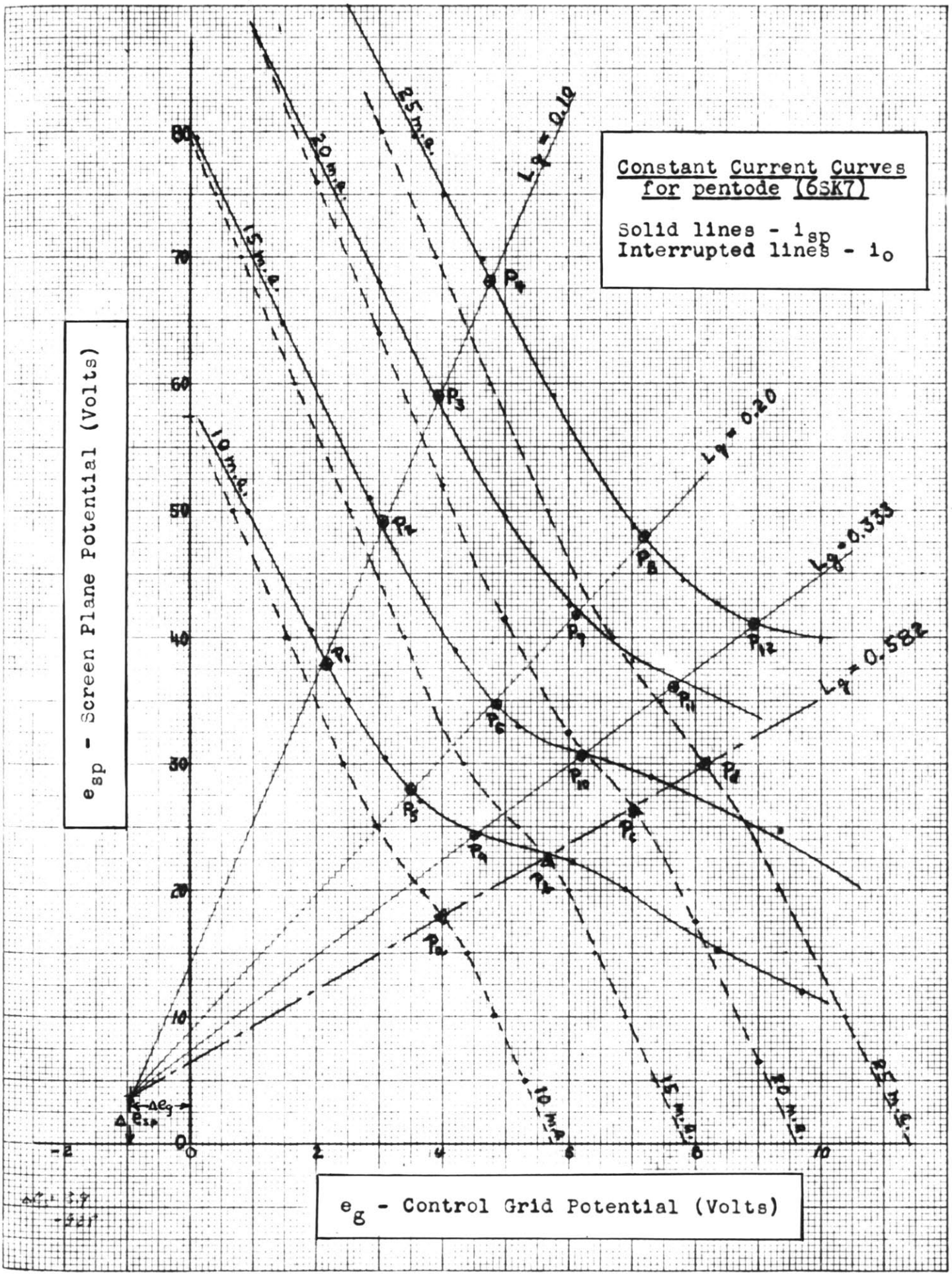
Constant Current Curves for pentode (6SK7)
Solid lines - i_{sp}
Interrupted lines - i_o
e_{sp} - Screen Plane Potential (Volts)
e_g - Control Grid Potential (Volts)
25 m.a.
20 m.a.
15 m.a.
10 m.a.
$L_g = 0.10$
$L_g = 0.20$
$L_g = 0.333$
$L_g = 0.582$
P_1
P_2
P_3
P_4
P_5
P_6
P_7
P_8
P_9
P_{10}
P_{11}
P_{12}
P_{13}
P_{14}
P_{15}
P_{16}
Δe_g
Δe_{sp}
-2
0
2
4
6
8
10
80
70
60
50
40
30
20
10
0

PLATE NO. III

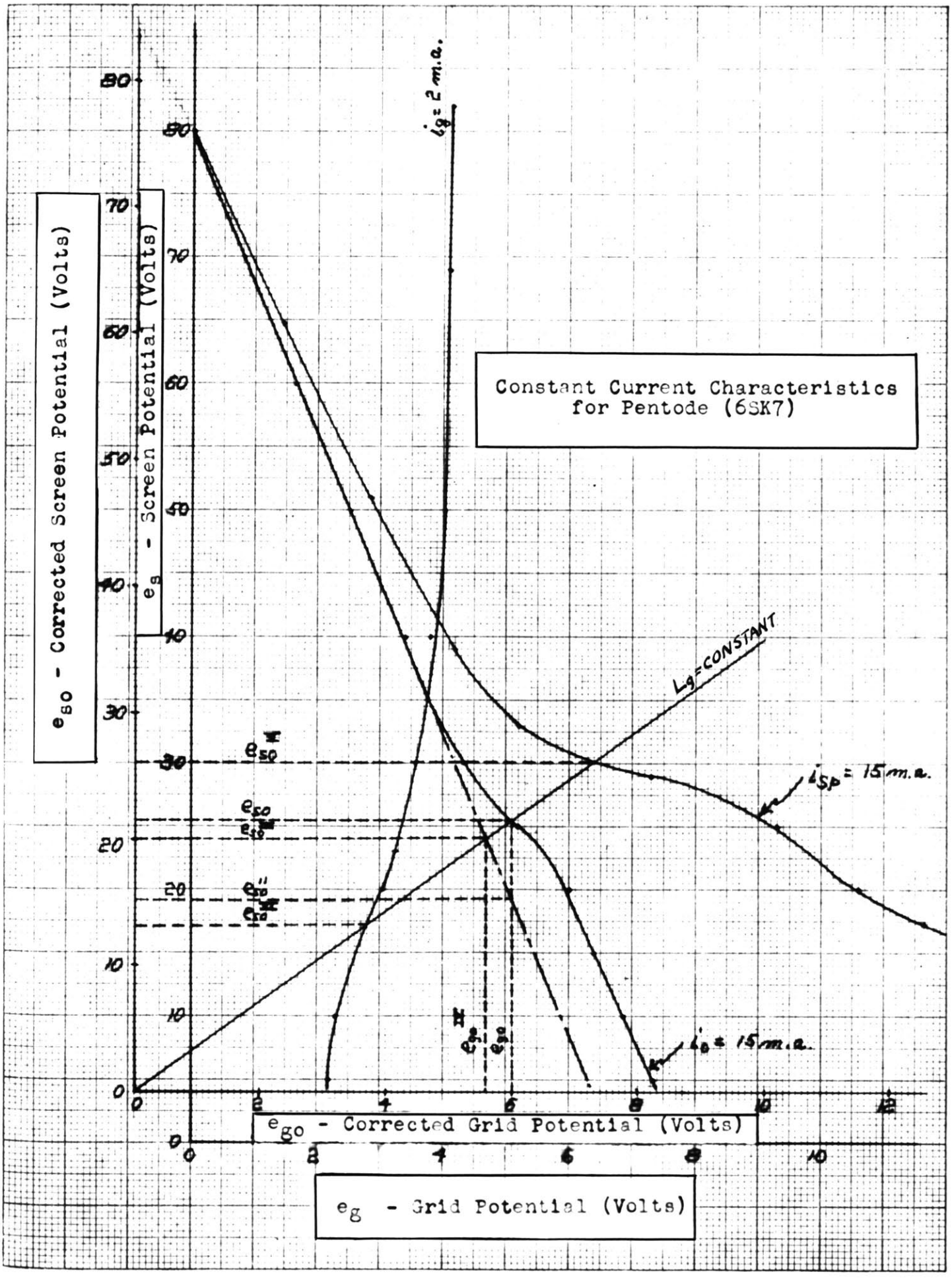
Constant Current Characteristics for Pentode (6SK7)
e_{so} - Corrected Screen Potential (Volts)
e_s - Screen Potential (Volts)
i_g = 2 m.a.
L_g = CONSTANT
i_{sp} = 15 m.a.
i_b = 15 m.a.
e_{go} - Corrected Grid Potential (Volts)
e_g - Grid Potential (Volts)

PLATE NO IV

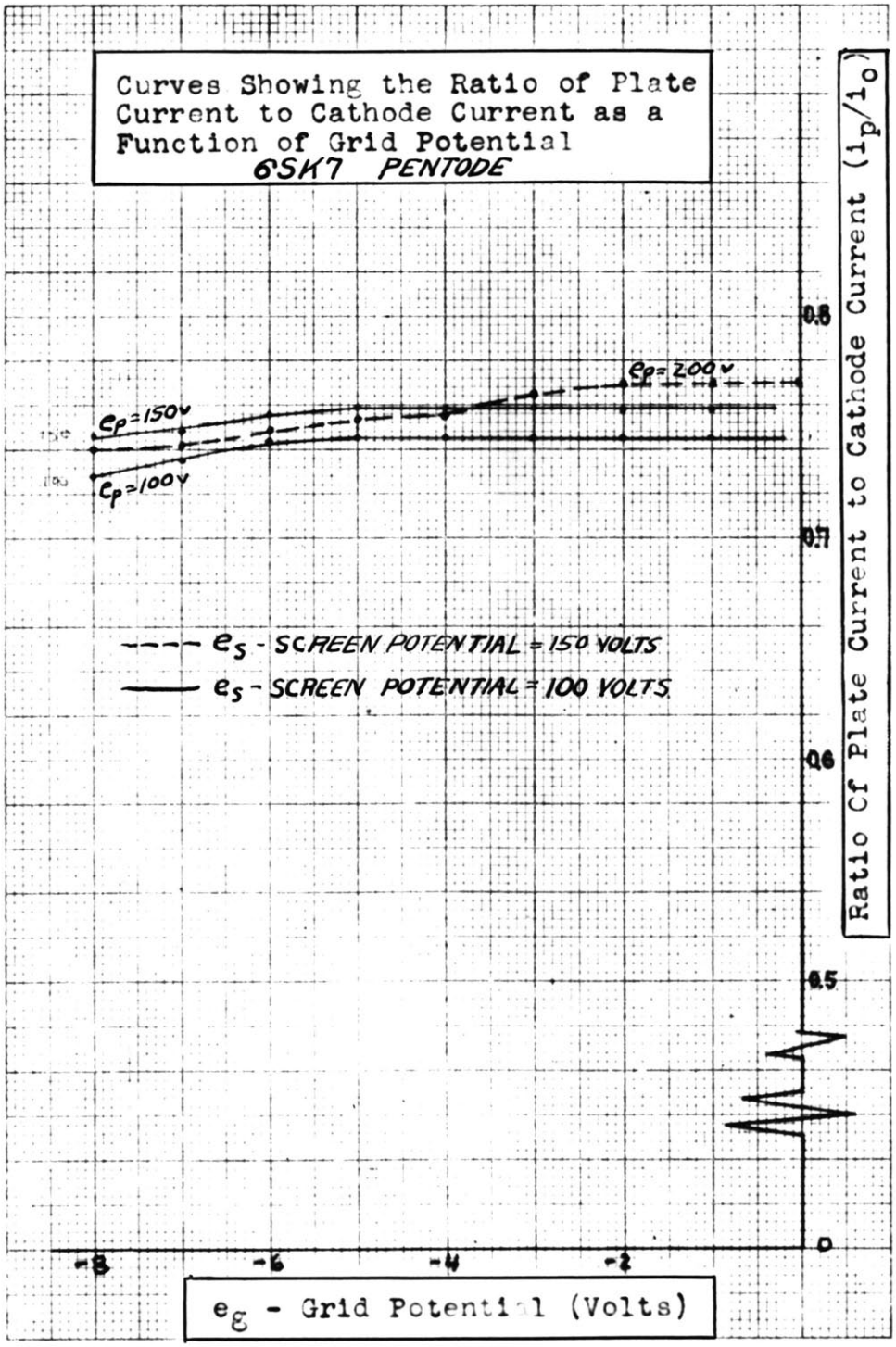
Curves Showing the Ratio of Plate Current to Cathode Current as a Function of Grid Potential
6SK7 PENTODE
Ratio Of Plate Current to Cathode Current (i_p/i_o)
0.8
0.7
0.6
0.5
0
e_p=200v
e_p=150v
e_p=100v
---- e_s - SCREEN POTENTIAL = 150 VOLTS
—— e_s - SCREEN POTENTIAL = 100 VOLTS
-8
-6
-4
-2
e_g - Grid Potential (Volts)

PLATE NO. V

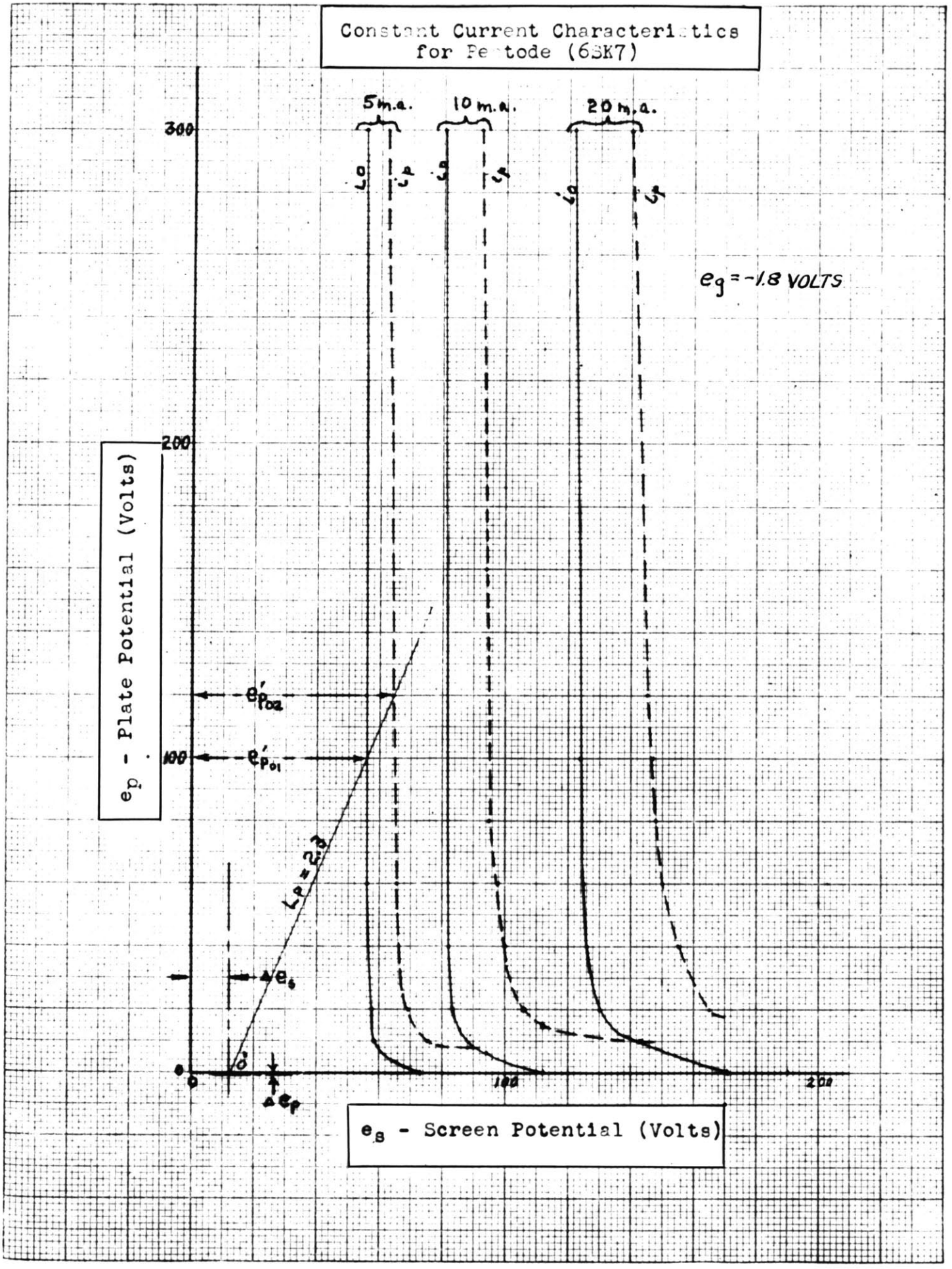
Constant Current Characteristics for Pentode (6SK7)
5 m.a.
10 m.a.
20 m.a.
e_g = -1.8 VOLTS
300
200
100
0
100
200
e_p - Plate Potential (Volts)
e_s - Screen Potential (Volts)
e'_{p02}
e'_{p01}
Δe_s
Δe_p
$\mu = 2.3$

PLATE NO. VI

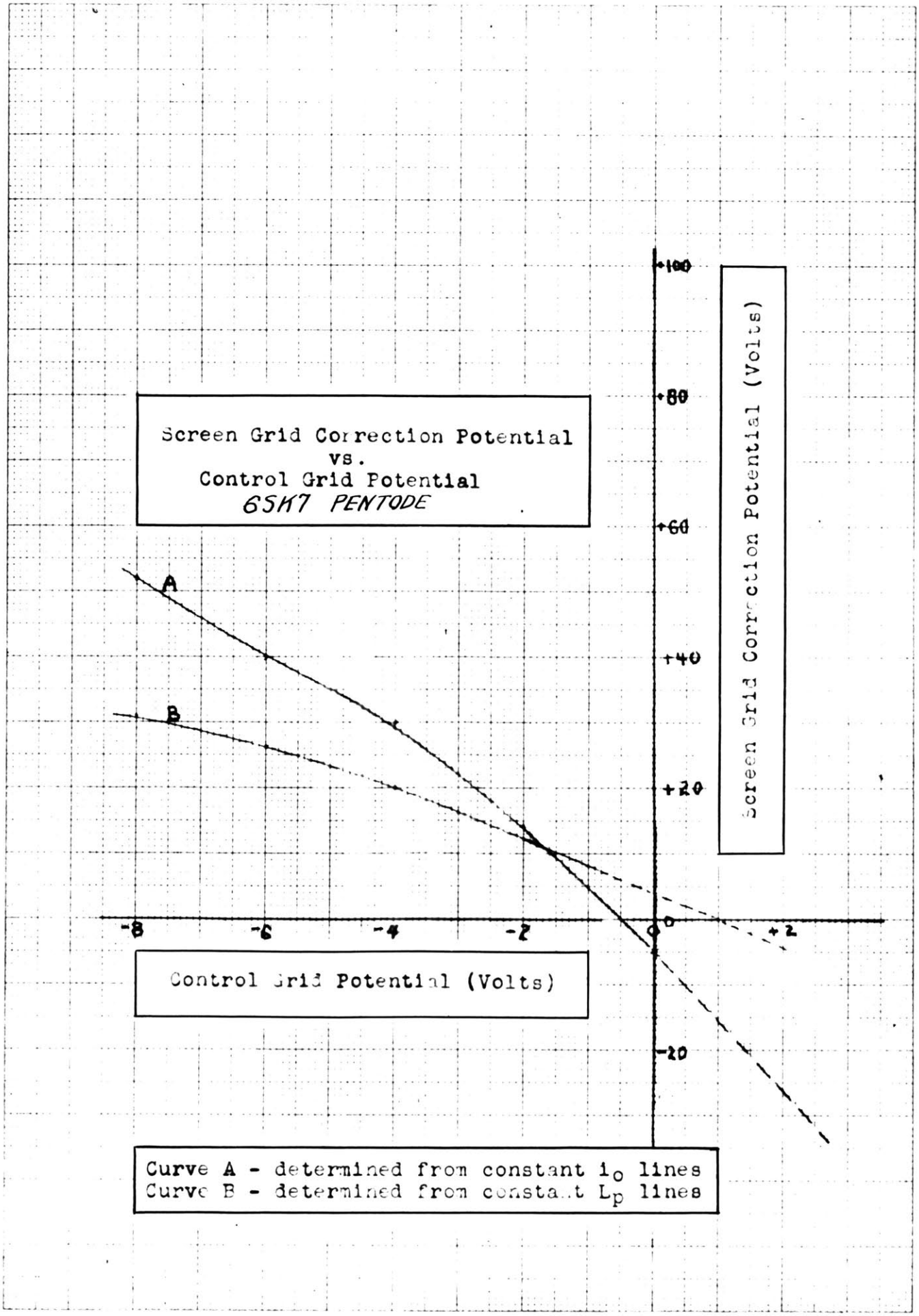
Screen Grid Correction Potential
vs.
Control Grid Potential
6SK7 PENTODE
+100
+80
+60
+40
+20
-20
Screen Grid Correction Potential (Volts)
A
B
-8
-6
-4
-2
0
+2
Control Grid Potential (Volts)
Curve A - determined from constant i_o lines
Curve B - determined from constant L_p lines

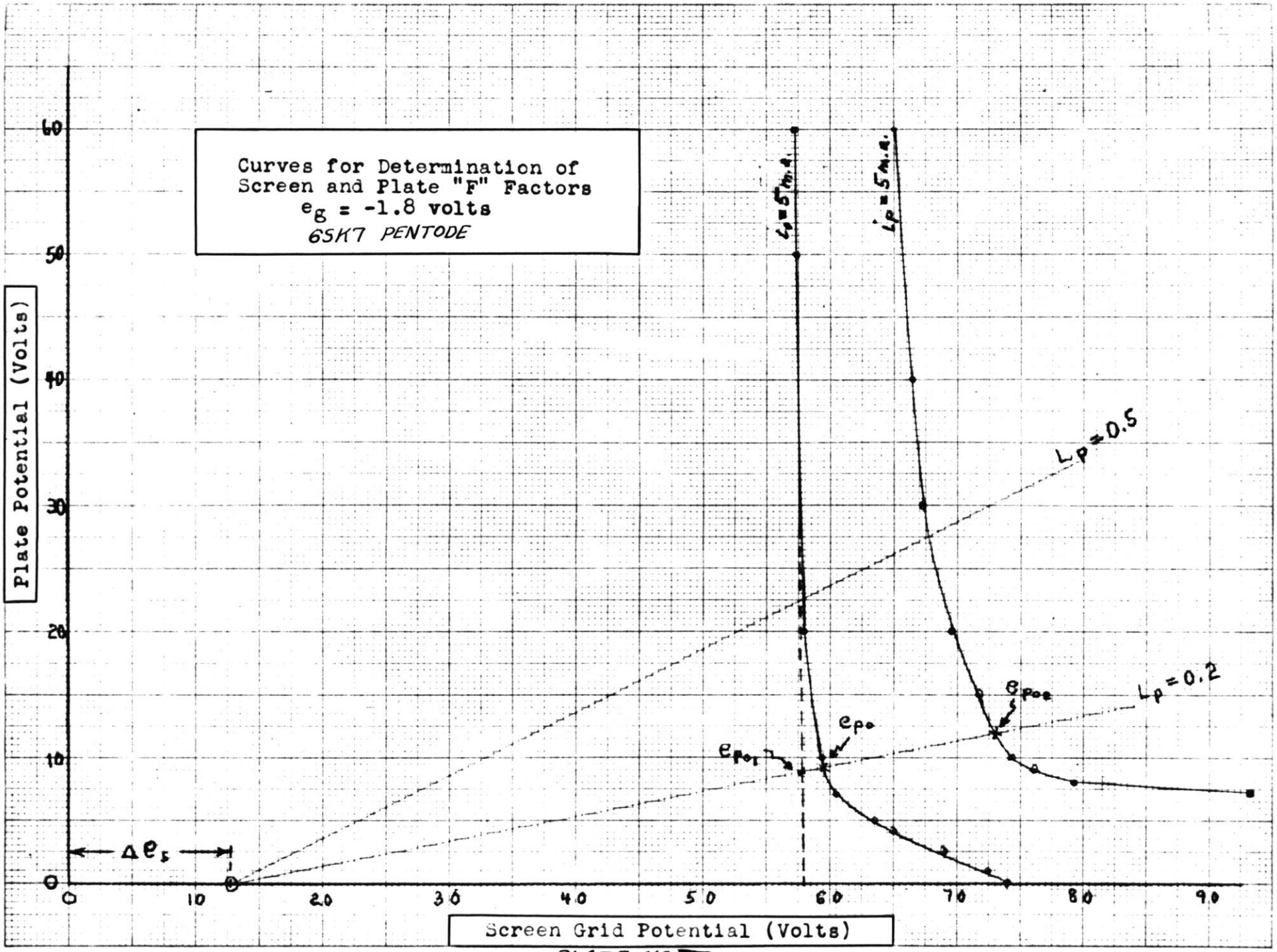
Curves for Determination of
Screen and Plate "F" Factors
e_g = -1.8 volts
6SK7 PENTODE
Plate Potential (Volts)
Screen Grid Potential (Volts)
i_p = 5 m.a.
i_p = 5 m.a.
L_p = 0.5
L_p = 0.2
e_{p_0}
$e_{p_{0_1}}$
$e_{p_{0_2}}$
Δe_s
0
10
20
30
40
50
60
70
80
90

PLATE NO VII

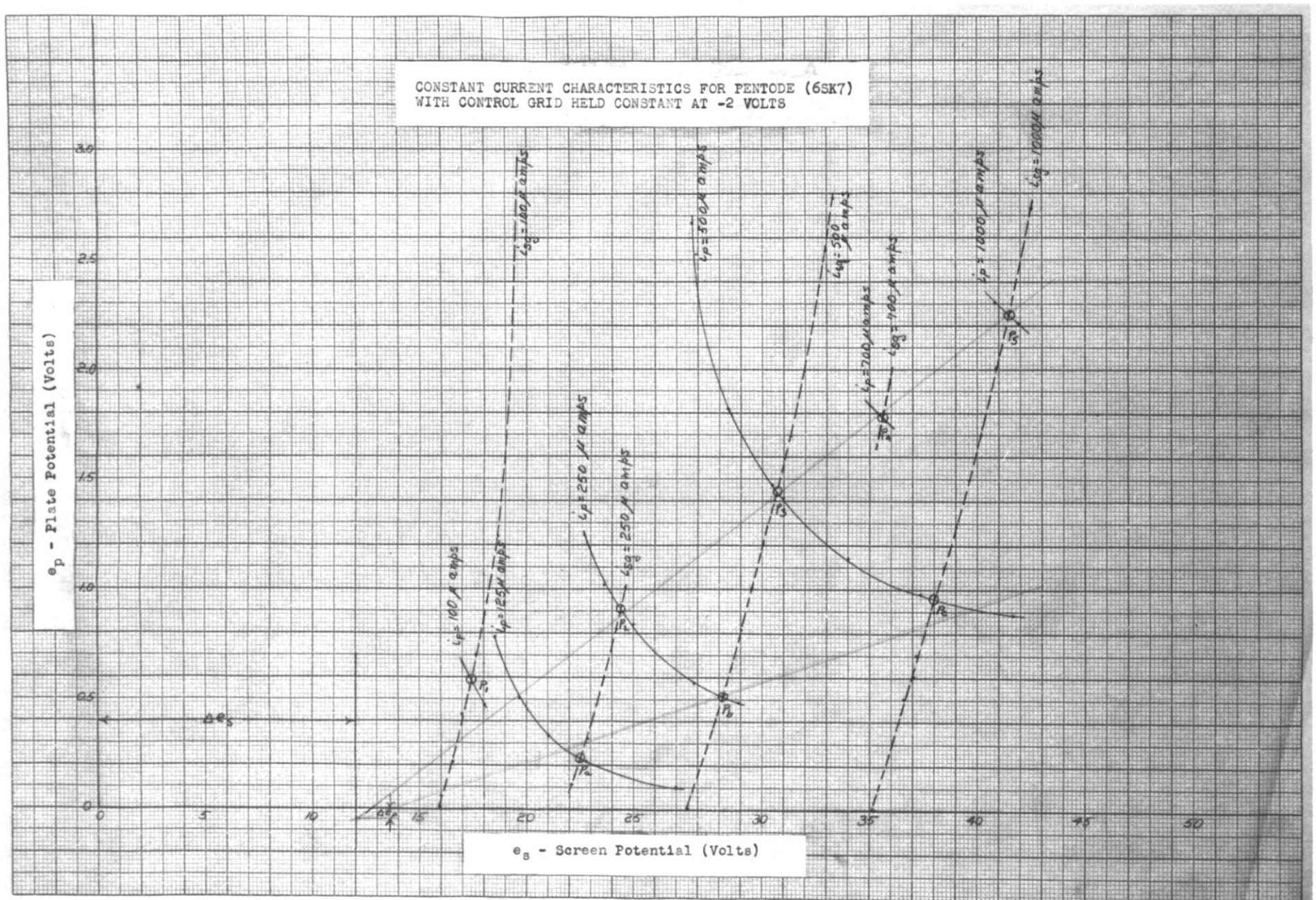

PLATE NO VIII

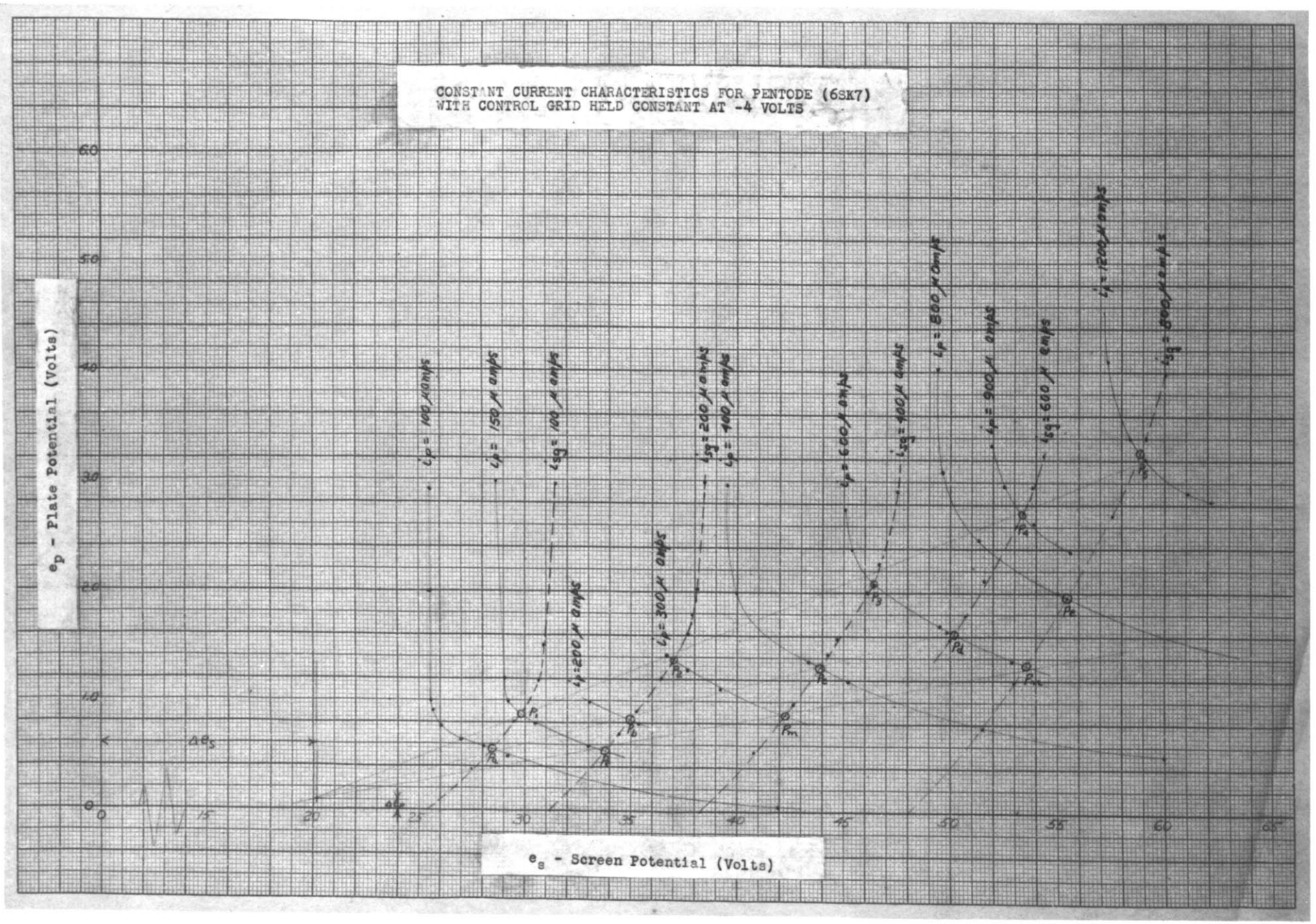
CONSTANT CURRENT CHARACTERISTICS FOR PENTODE (6SK7)
WITH CONTROL GRID HELD CONSTANT AT -4 VOLTS
e_p - Plate Potential (Volts)
e_s - Screen Potential (Volts)
Δe_s
$\frac{\Delta e_s}{\Delta e_k}$
i_p = 100 μamps
i_p = 150 μamps
i_p = 200 μamps
i_p = 300 μamps
i_p = 400 μamps
i_p = 600 μamps
i_p = 800 μamps
i_p = 1200 μamps
i_{s_1}
i_{s_2}
i_{s_3}
i_{s_4}
i_{s_5}
i_{s_6}
i_{s_7}
i_{s_8}
0
10
20
30
40
50
60
70
15
25
35
45
55
65

PLATE NO. IX

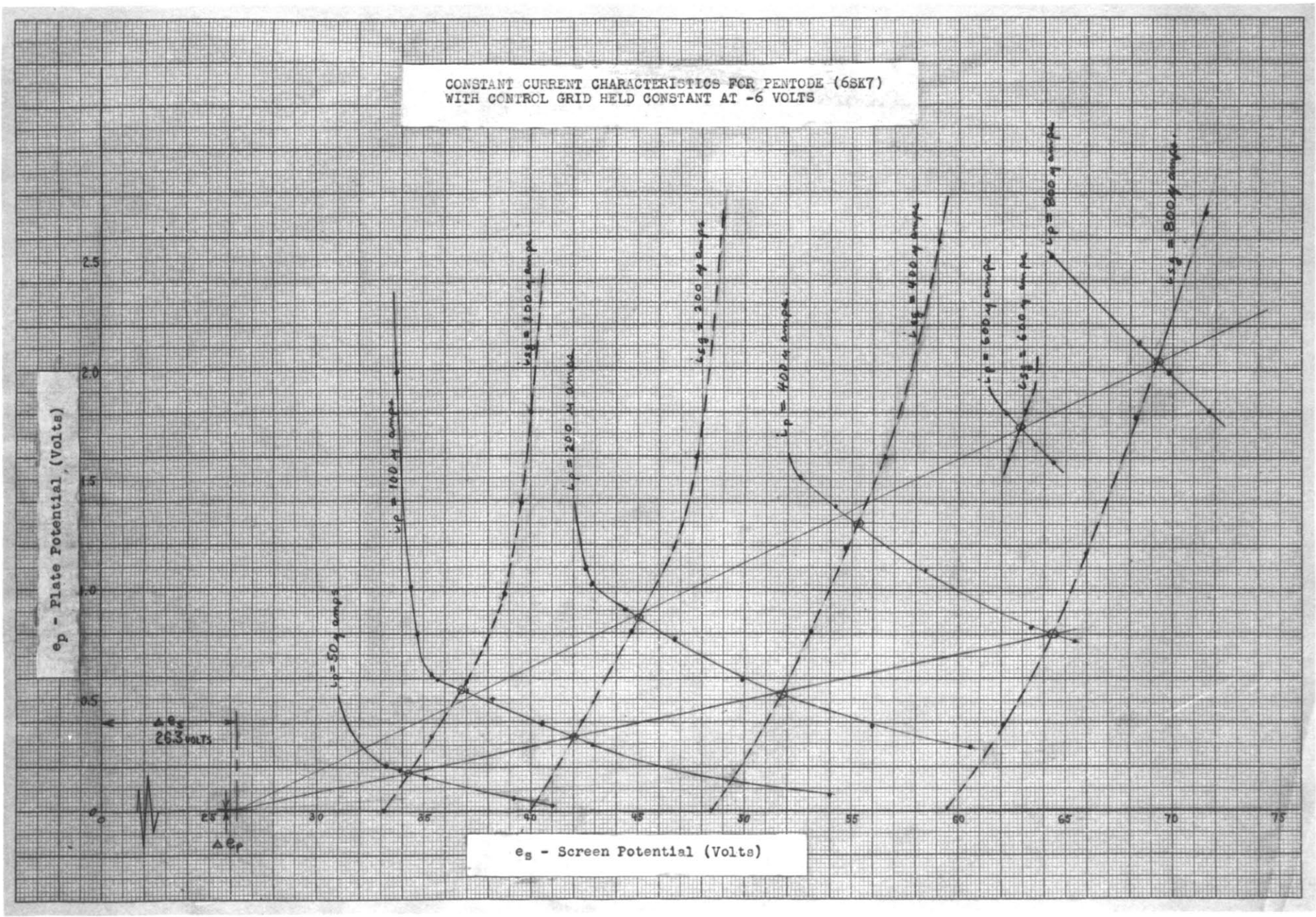
CONSTANT CURRENT CHARACTERISTICS FOR PENTODE (6SK7)
WITH CONTROL GRID HELD CONSTANT AT -6 VOLTS
e_p - Plate Potential (Volts)
e_s - Screen Potential (Volts)
i_p = 50 μ amps
i_p = 100 μ amps
i_p = 200 μ amps
i_p = 400 μ amps
i_p = 600 μ amps
i_p = 800 μ amps
i_{cg} = 100 μ amps
i_{cg} = 200 μ amps
i_{cg} = 400 μ amps
i_{cg} = 600 μ amps
i_{cg} = 800 μ amps
Δe_s 26.3 VOLTS
Δe_p
2.5
2.0
1.5
1.0
0.5
0
25
30
35
40
45
50
55
60
65
70
75

PLATE NO X

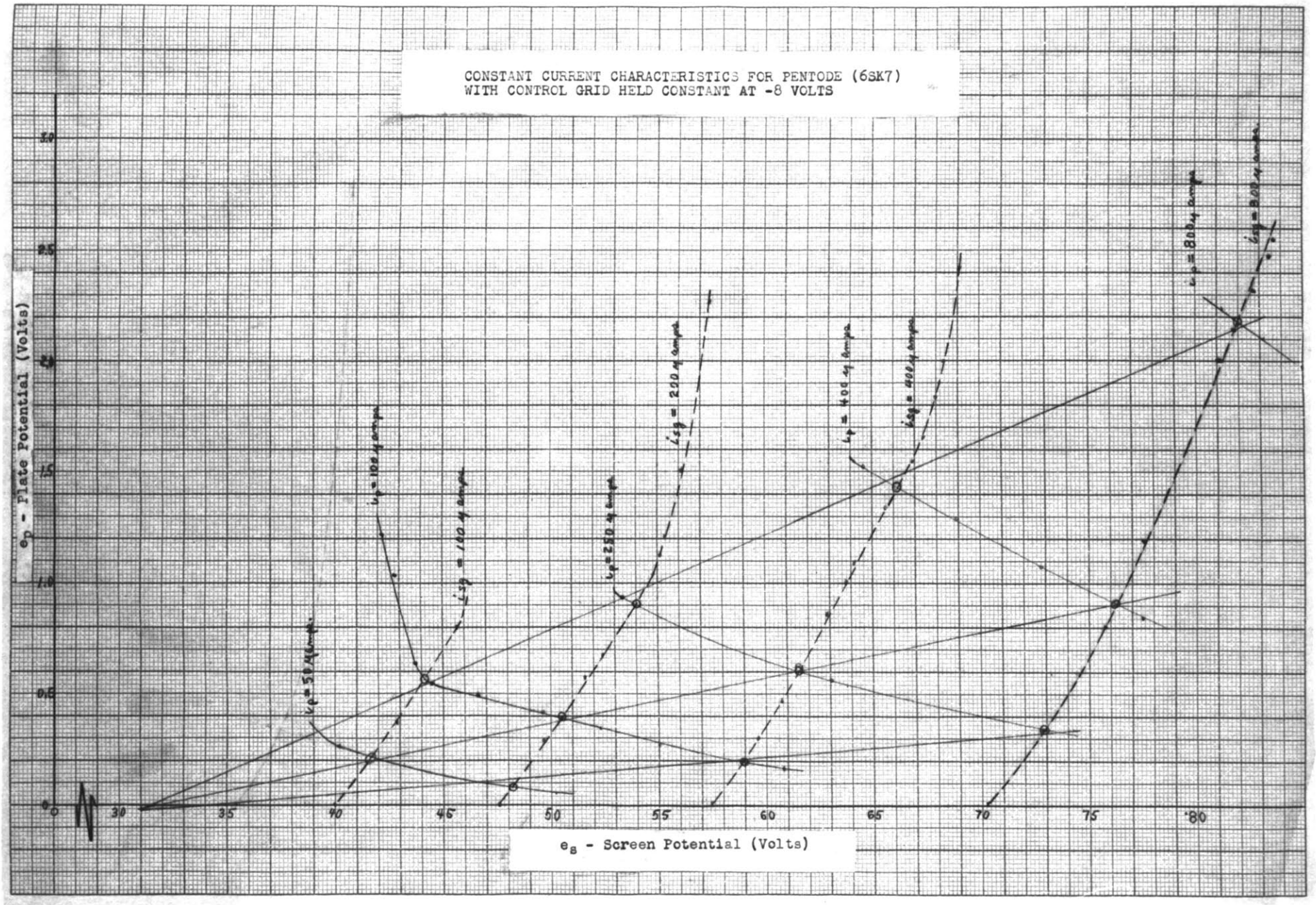
CONSTANT CURRENT CHARACTERISTICS FOR PENTODE (6SK7)
WITH CONTROL GRID HELD CONSTANT AT -8 VOLTS
e_p - Plate Potential (Volts)
e_g - Screen Potential (Volts)
i_p = 50 Microamps.
i_p = 100 Microamps.
i_p = 200 Microamps.
i_p = 400 Microamps.
i_p = 800 Microamps.
i_{sg} = 100 Microamps.
i_{sg} = 200 Microamps.
i_{sg} = 400 Microamps.
i_{sg} = 800 Microamps.
0
30
35
40
45
50
55
60
65
70
75
80

PLATE NO. XI

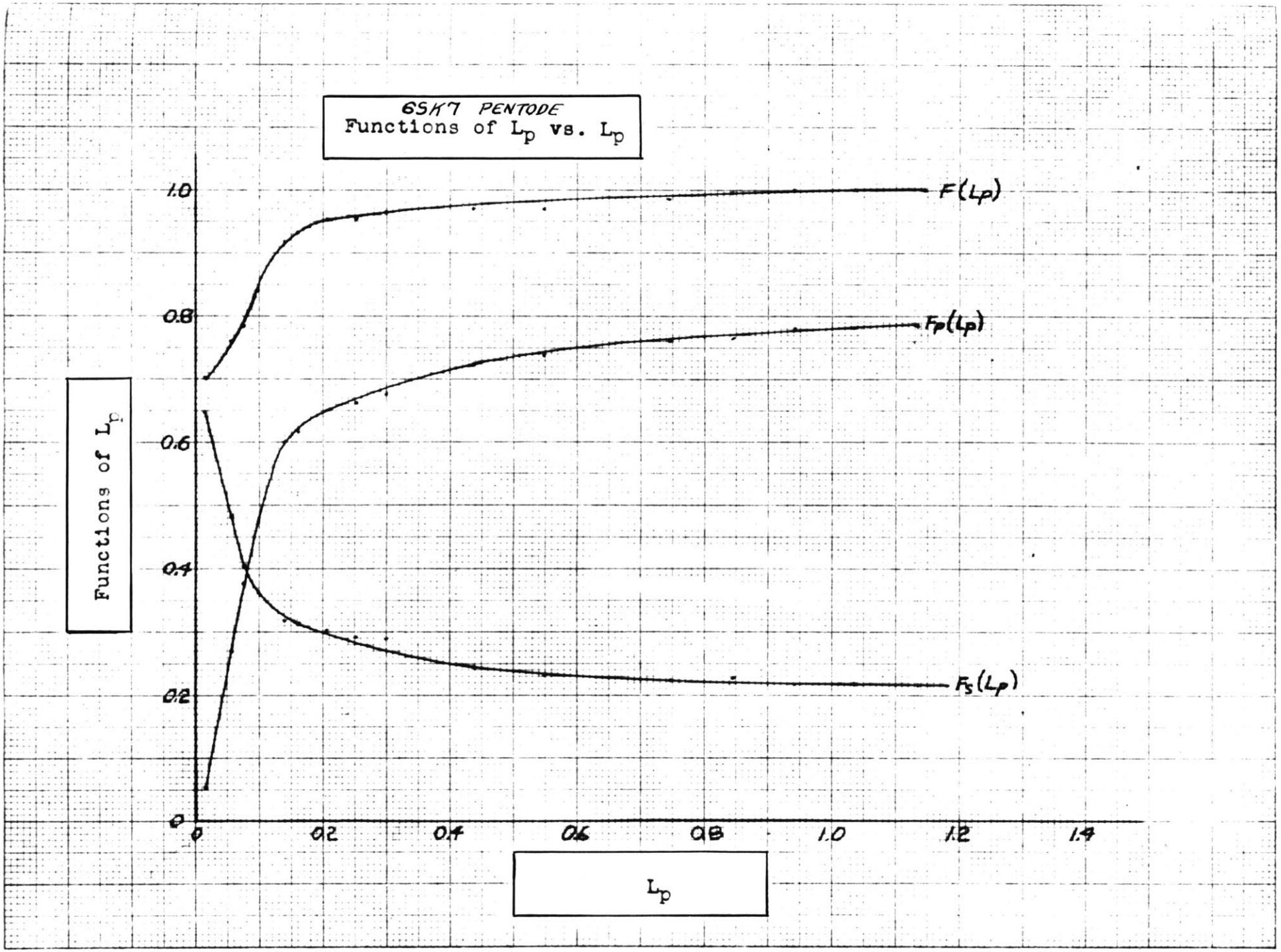
6SK7 PENTODE
Functions of L_p vs. L_p
Functions of L_p
1.0
0.8
0.6
0.4
0.2
0
0
0.2
0.4
0.6
0.8
1.0
1.2
1.4
L_p
$F(L_p)$
$F_p(L_p)$
$F_s(L_p)$

PLATE NO. XII

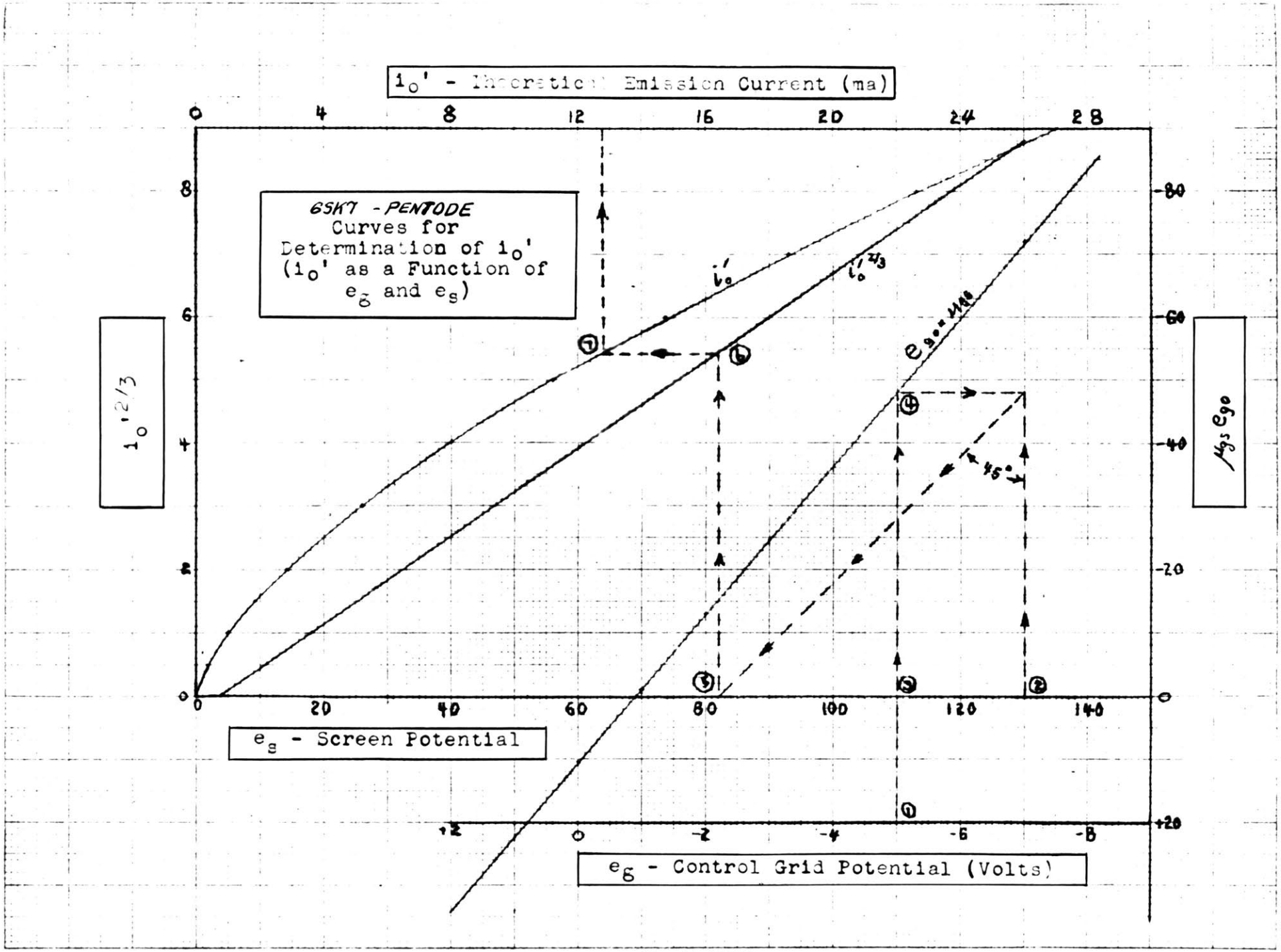

PLATE NO XIII

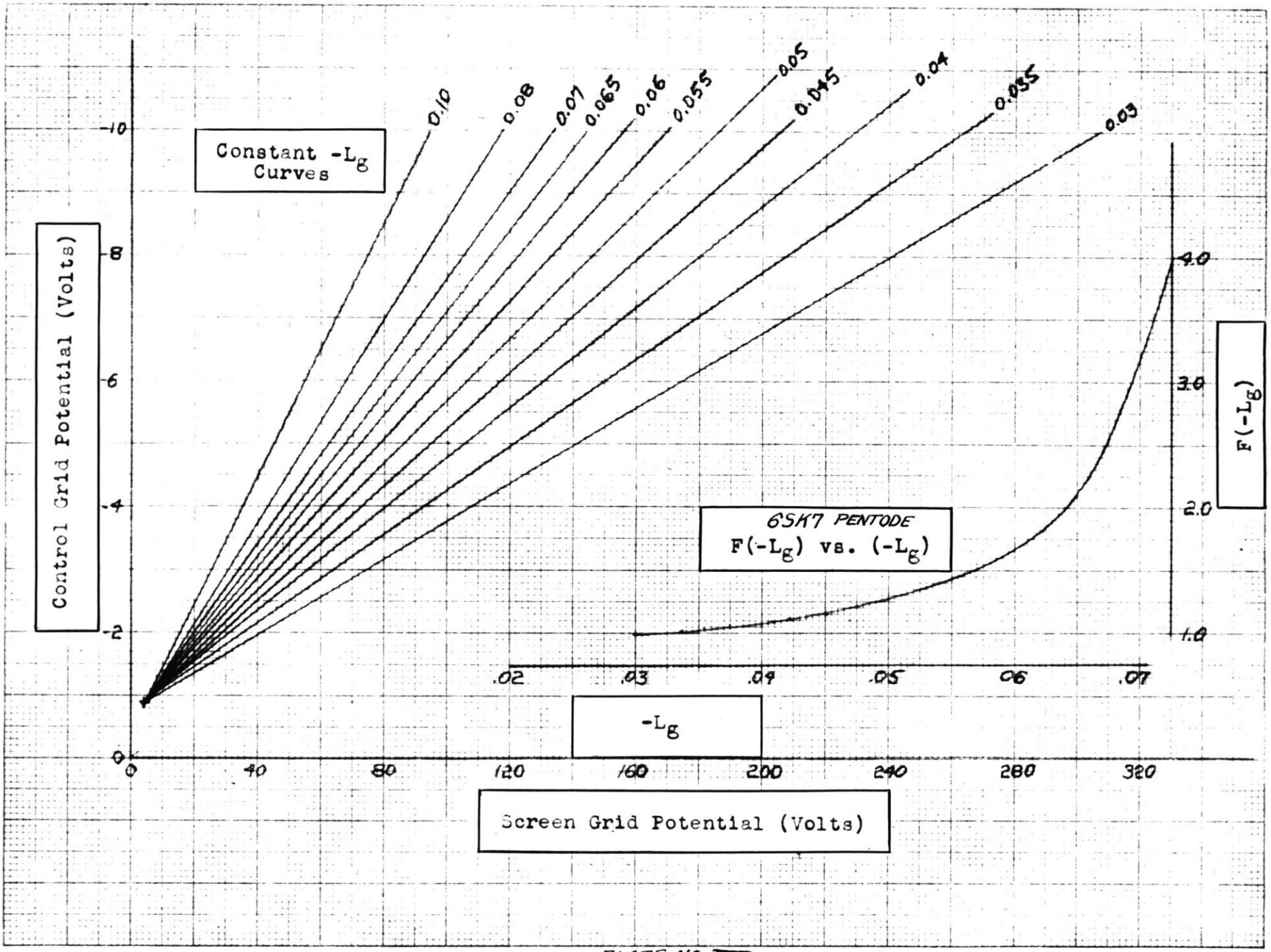
Constant -Lg Curves
0.10
0.08
0.07
0.065
0.06
0.055
0.05
0.045
0.04
0.035
0.03
Control Grid Potential (Volts)
-10
-8
-6
-4
-2
0
6SK7 PENTODE
F(-Lg) vs. (-Lg)
4.0
3.0
2.0
1.0
F(-Lg)
.02
.03
.04
.05
.06
.07
-Lg
0
40
80
120
160
200
240
280
320
Screen Grid Potential (Volts)

PLATE NO. XIV

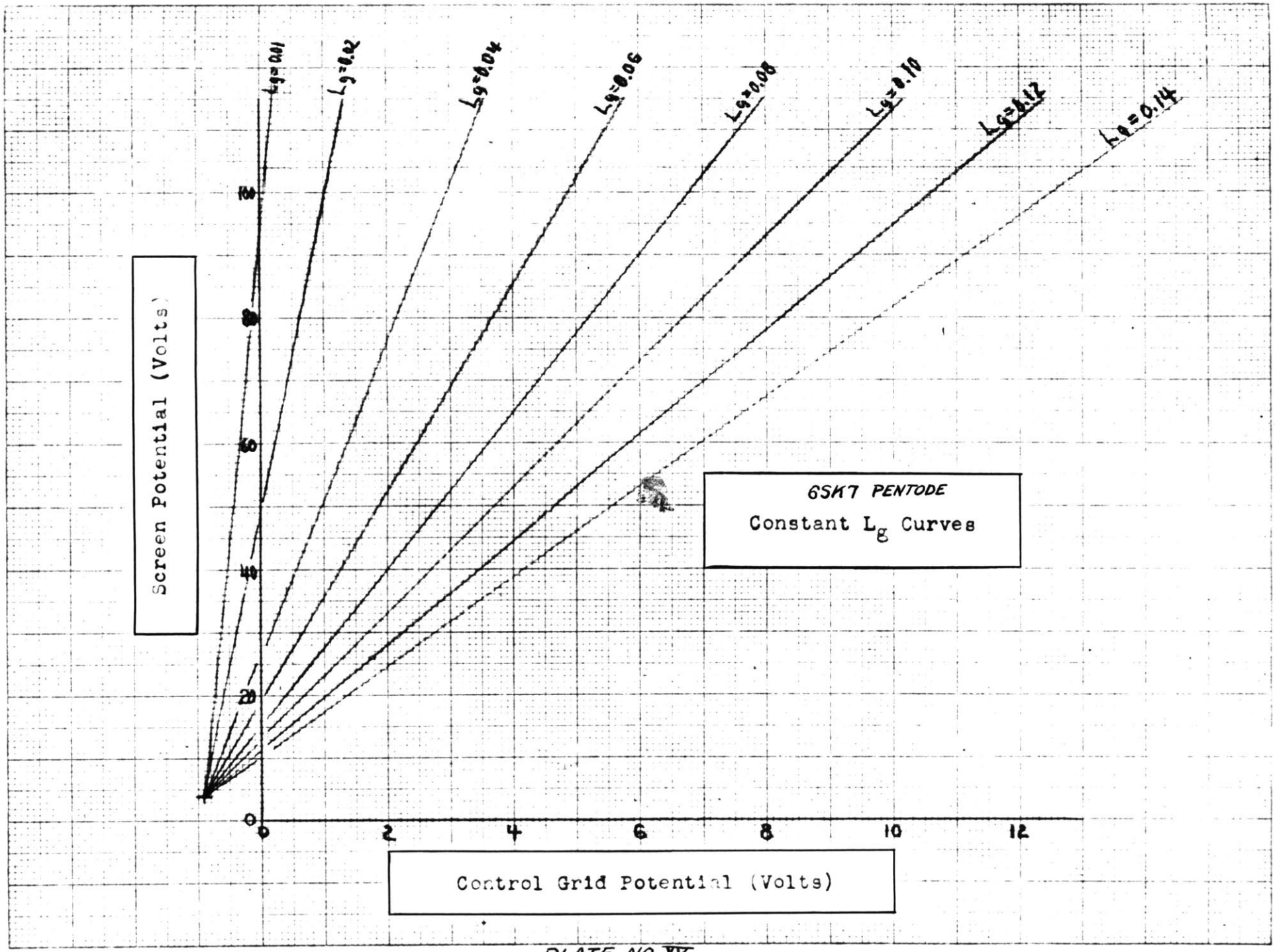
Lg=0.01
Lg=0.02
Lg=0.04
Lg=0.06
Lg=0.08
Lg=0.10
Lg=0.12
Lg=0.14
100
80
60
40
20
0
0
2
4
6
8
10
12
Screen Potential (Volts)
Control Grid Potential (Volts)
6SK7 PENTODE
Constant Lg Curves

PLATE NO. XV

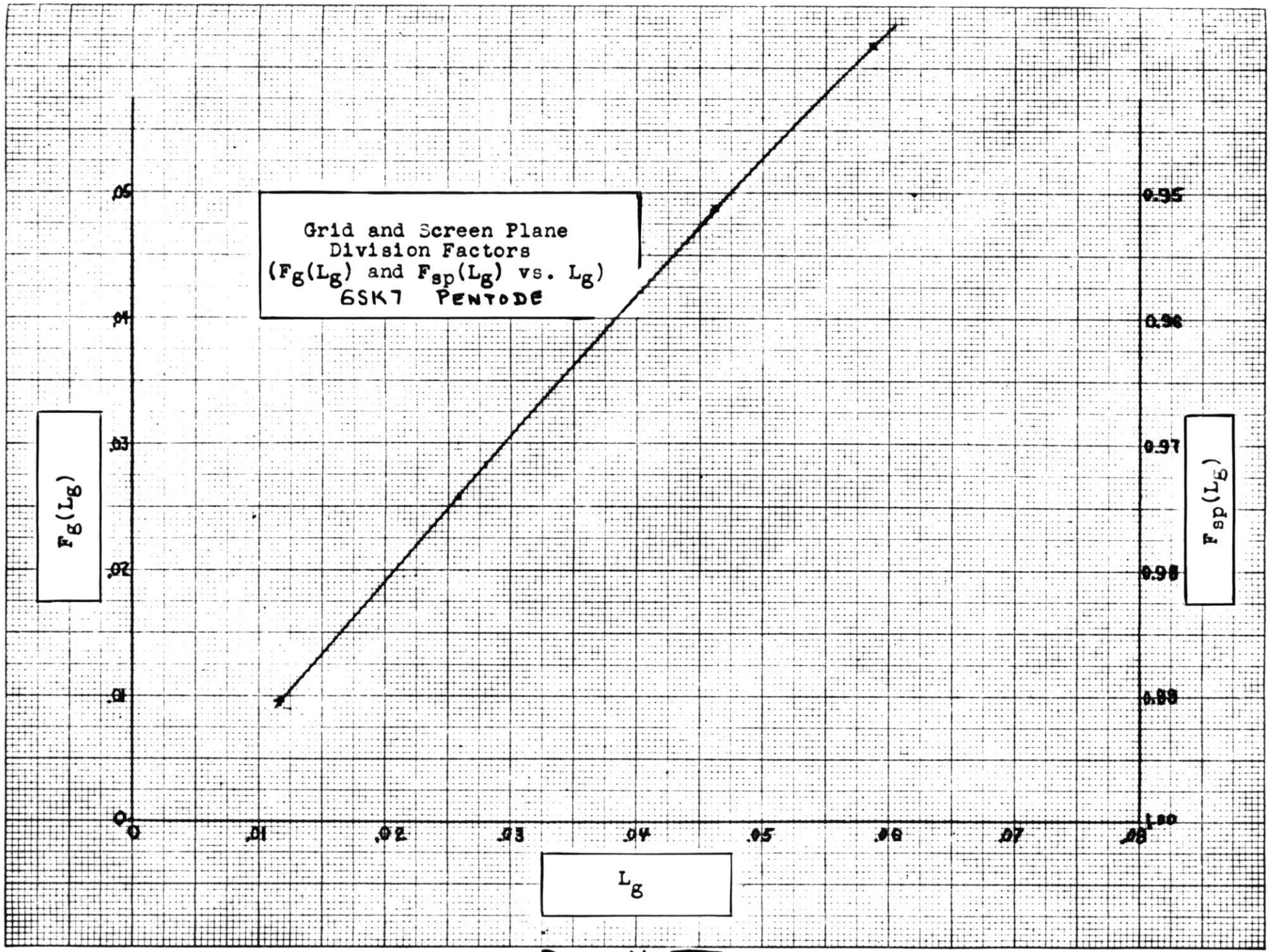
Grid and Screen Plane
Division Factors
($F_g(L_g)$ and $F_{sp}(L_g)$ vs. L_g)
6SK7 PENTODE
$F_g(L_g)$
$F_{sp}(L_g)$
L_g
0
.01
.02
.03
.04
.05
.06
.07
.08
0.95
0.96
0.97
0.98
0.99
1.00

PLATE No. XVI

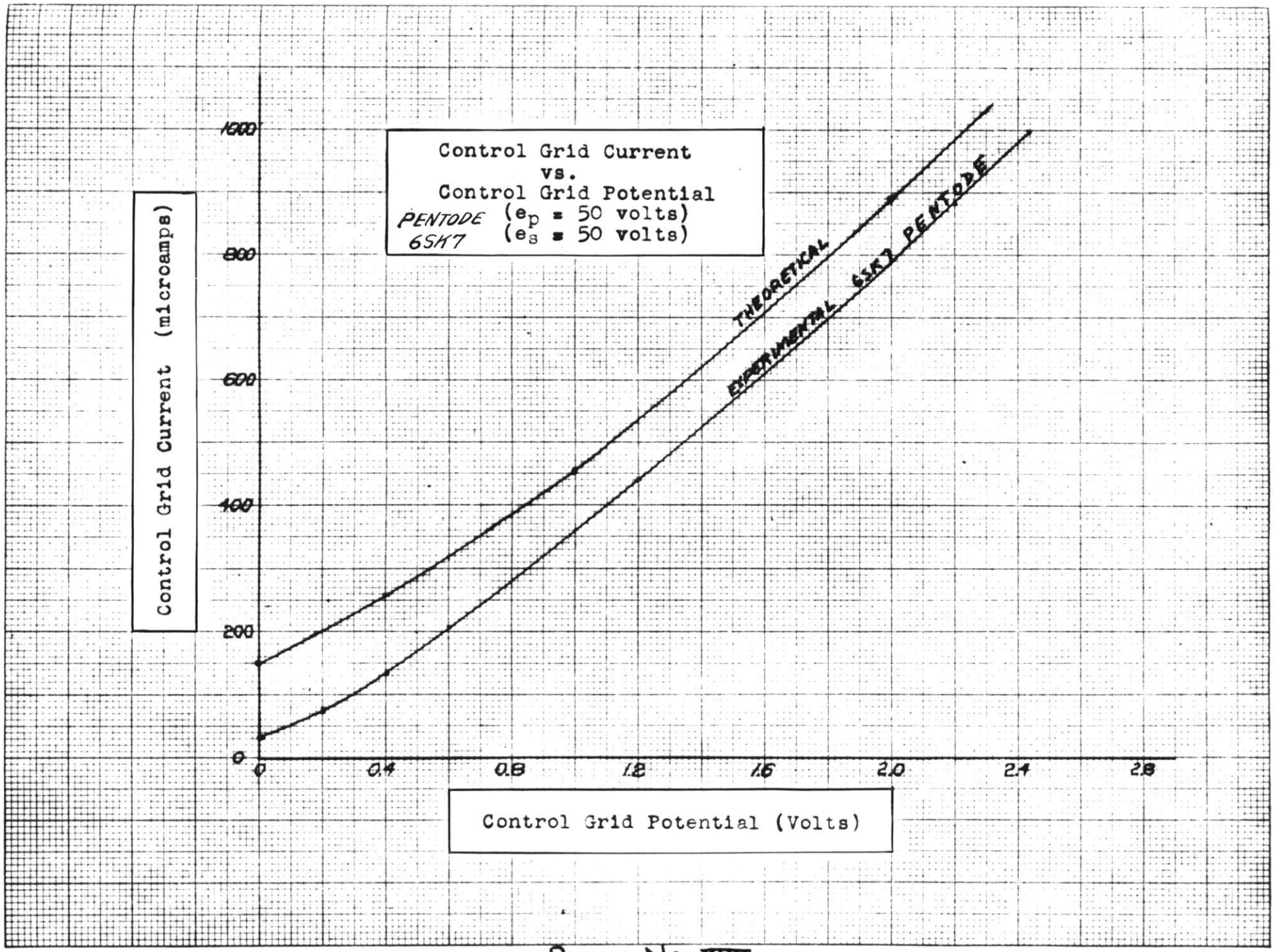

PLATE NO. XVII

PLATE NO. XVIII

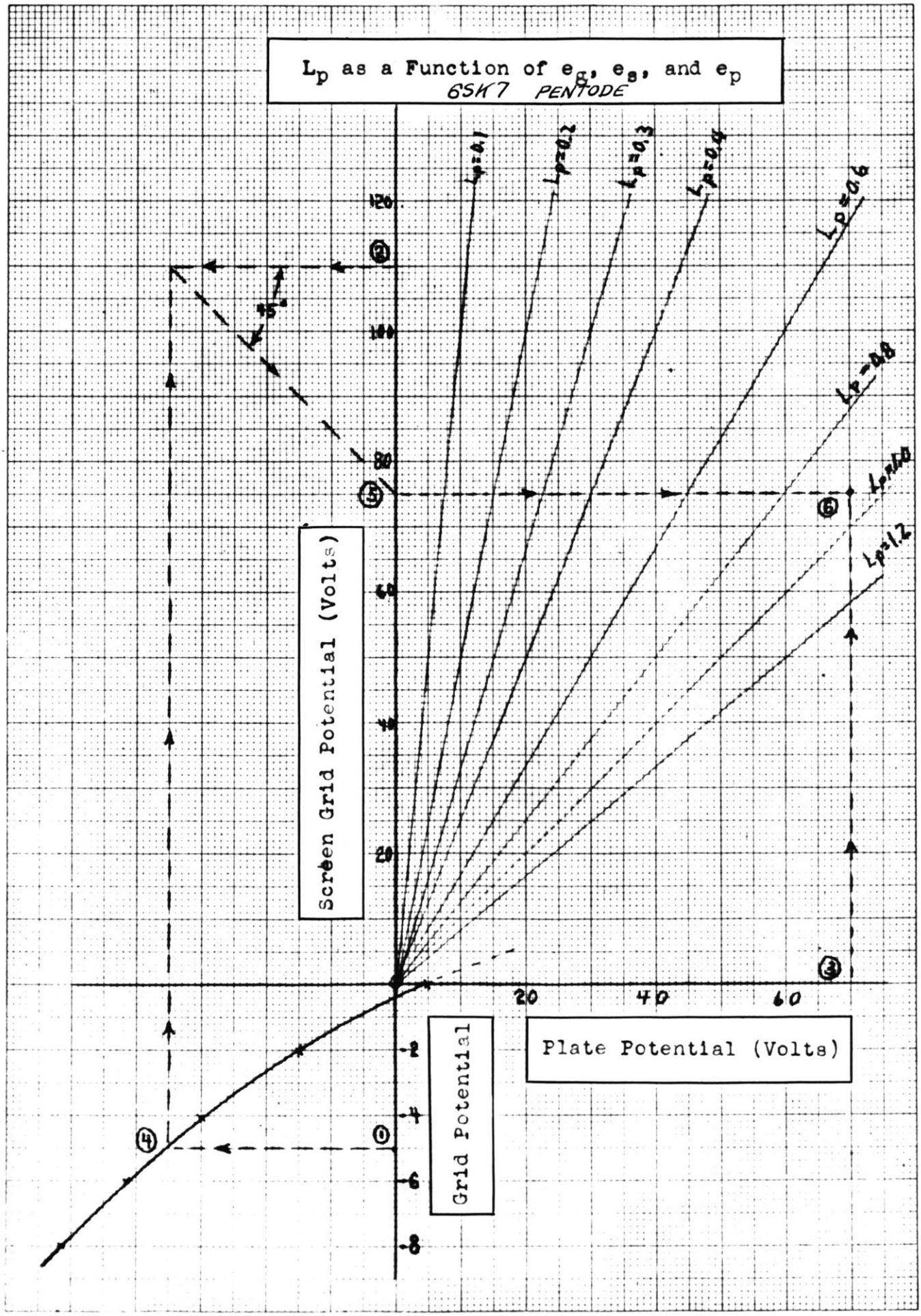

PLATE NO. XIX

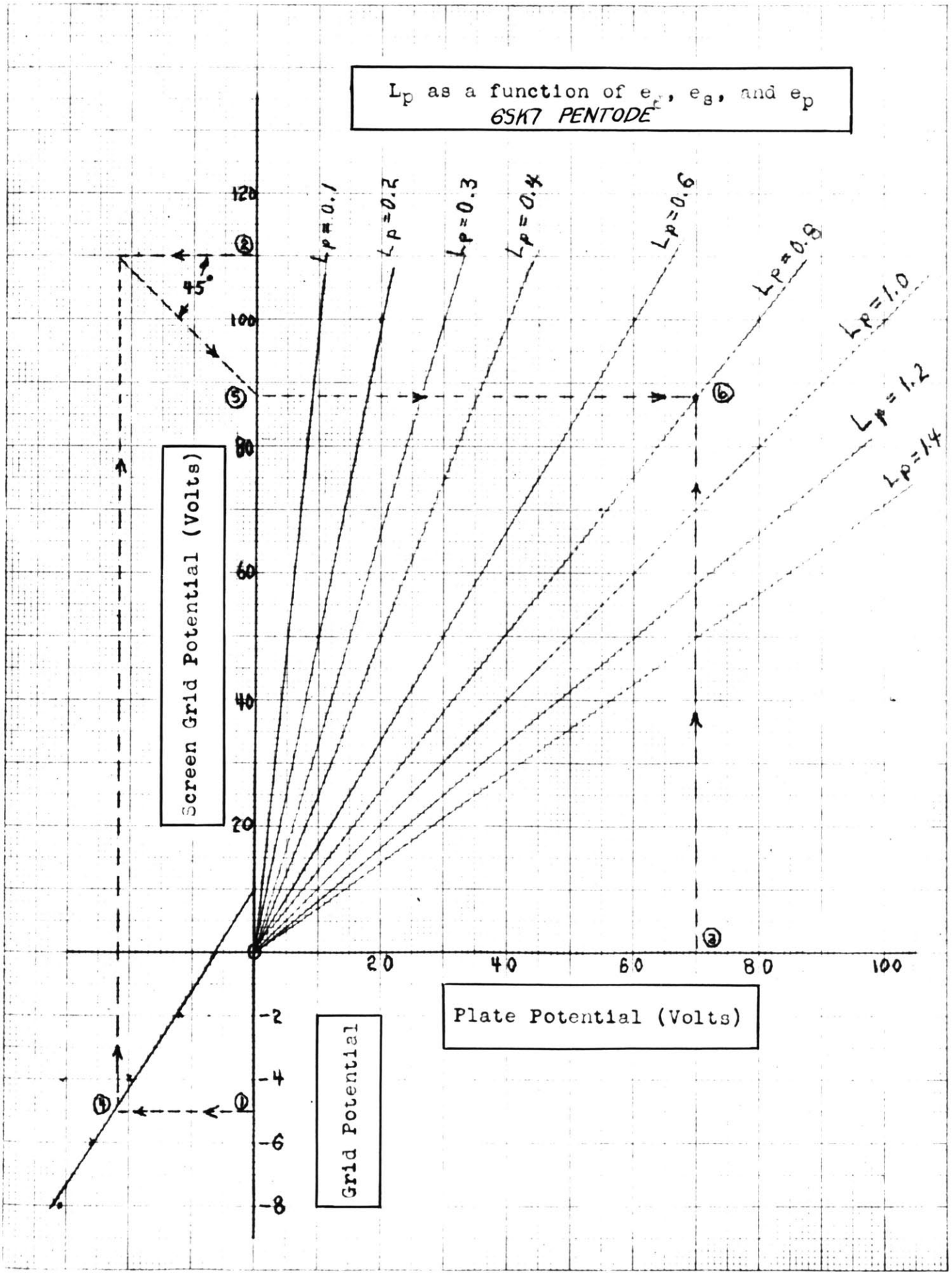
L_p as a function of e_g, e_s, and e_p
6SK7 PENTODE
L_p=0.1
L_p=0.2
L_p=0.3
L_p=0.4
L_p=0.6
L_p=0.8
L_p=1.0
L_p=1.2
L_p=1.4
Screen Grid Potential (Volts)
120
100
80
60
40
20
45°
Plate Potential (Volts)
20
40
60
80
100
Grid Potential
-2
-4
-6
-8
1
2
3
4
5
6

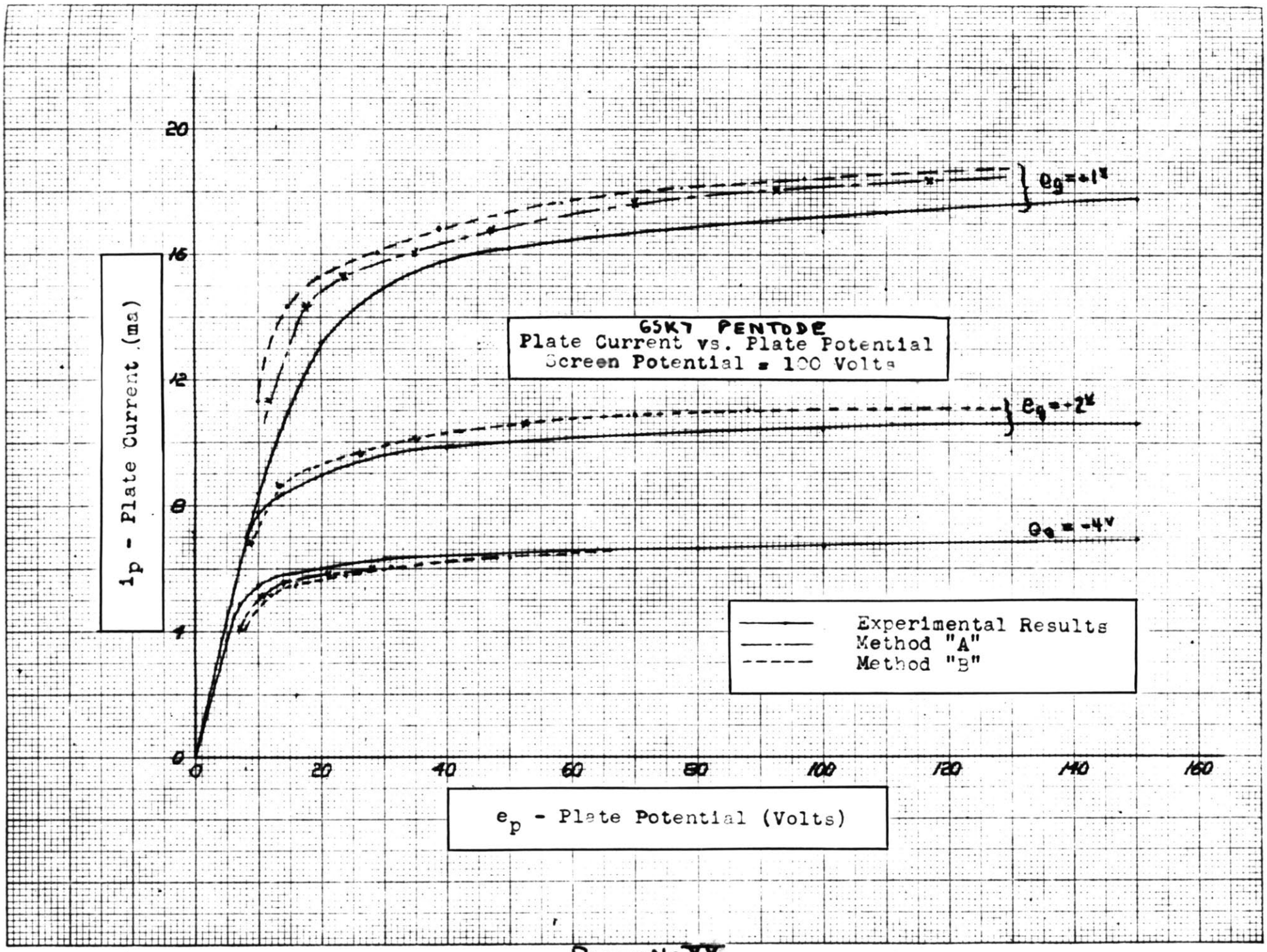
6SK7 PENTODE
Plate Current vs. Plate Potential
Screen Potential = 100 Volts
i_p - Plate Current (ma)
e_p - Plate Potential (Volts)
e_g = +1V
e_g = +2V
e_g = -4V
Experimental Results
Method "A"
Method "B"
0
4
8
12
16
20
0
20
40
60
80
100
120
140
160

PLATE No. XX

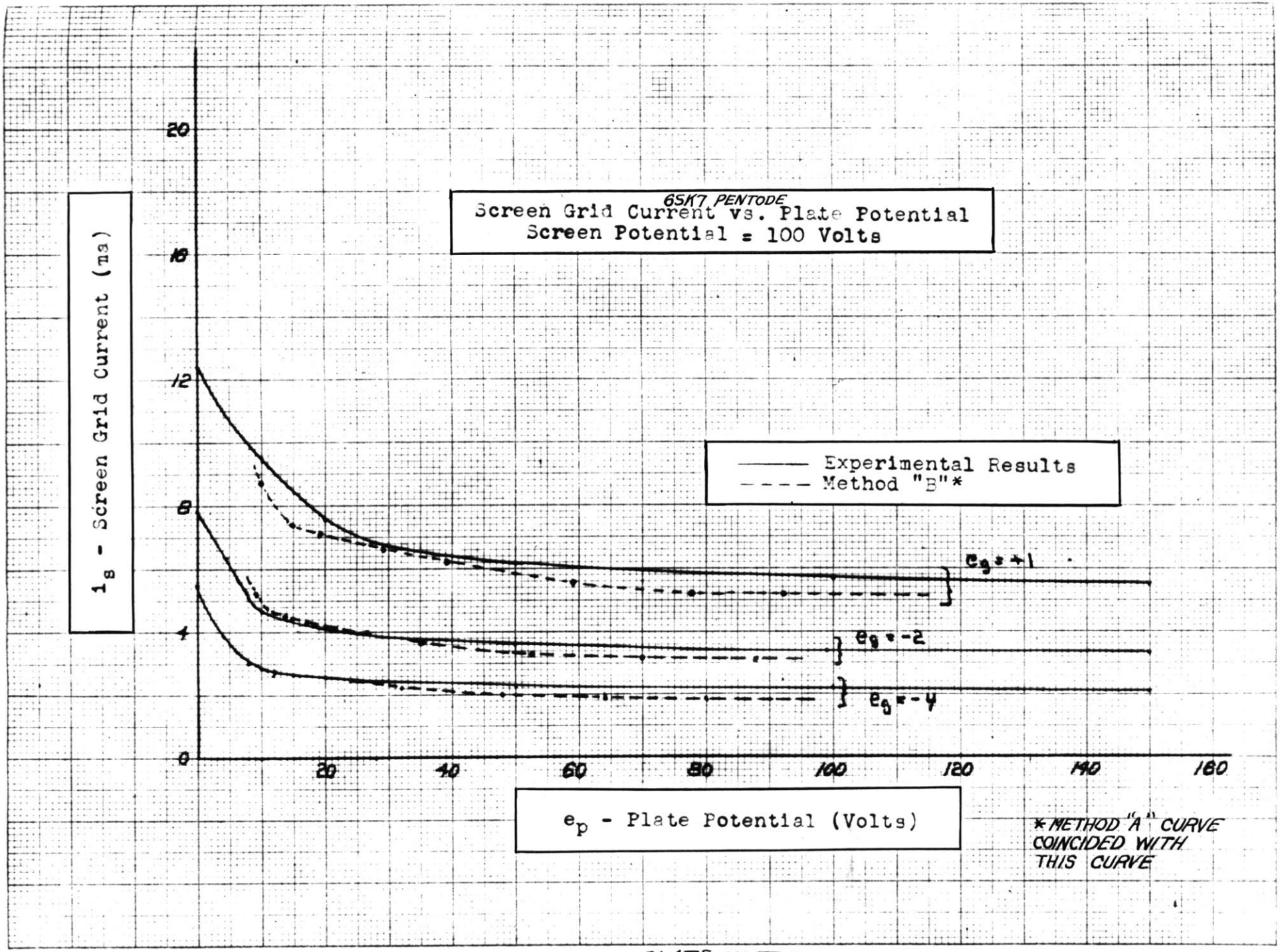
6SK7 PENTODE
Screen Grid Current vs. Plate Potential
Screen Potential = 100 Volts
i_s - Screen Grid Current (ma)
20
16
12
8
4
0
20
40
60
80
100
120
140
160
Experimental Results
Method "B"*
e_g = +1
e_g = -2
e_g = -4
e_p - Plate Potential (Volts)
*METHOD "A" CURVE COINCIDED WITH THIS CURVE

PLATE NO. XXI

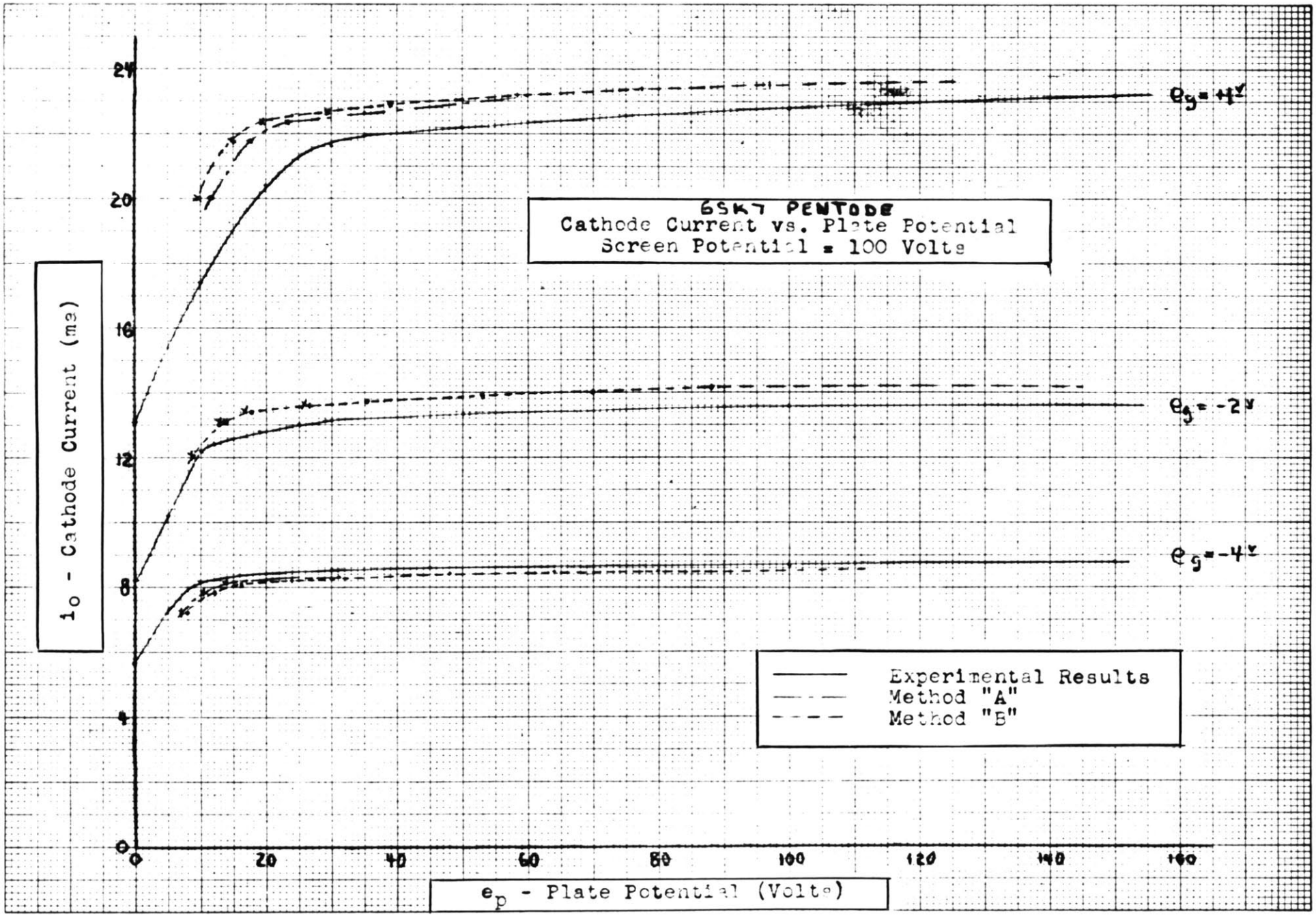

PLATE No. XXII